APPENDIX F

Probabilistic Seismic Hazard Assessment

Table of Contents

LIST OF TABLES

LIST OF FIGURES

1.0 Introduction and Summary

A site-specific probabilistic seismic hazard assessment (PSHA) was performed for the planned Eagle Rock Enrichment Facility (EREF) to be sited in Bonneville County Idaho. The site is located at the following geographic coordinates.

112.4400^{O} W. Longitude

43.5909^{O} N. Latitude

Seismic ground motion amplitudes in bedrock were determined for annual frequencies of exceedance ranging from of 10^{-2} to 10^{-5}. Uniform hazard response spectra (UHRS) were determined for top of bedrock for annual frequencies of exceedance of 2.1 x 10^{-3}, 10^{-3}, 10^{-4}, and 10^{-5}.

The site is situated in a less seismically active region of the Eastern Snake River Plain (ESRP). Introduction and solidification of molten volcanic materials in ESRP fracture zones as they developed in the past is believed to be a possible mechanism responsible for the present low level of seismic activity (Parsons and Thompson, 1991). Most of the areas to the north, east, and south of the ESRP experience earthquake activity along faults related to regional Basin and Range crustal extension; the ESRP, however, is an area of low present-day seismicity. The PSHA models the site region to be composed of a less seismically active ESRP surrounded by more seismically active Basin and Range provinces and faulted terrain.

Uniform hazard response spectra were determined for the top of basalt bedrock. The uppermost 30.5 m (100 ft) of bedrock material is estimated to have a shear wave velocity of approximately 1,400 m/sec (4,700 ft/sec) based on regional geophysical measurements in ESRP bedrock (Payne et al. 2002). The EREF site most likely has a bedrock shear wave velocity that is equal to but more likely greater than the National Earthquake Hazards Reduction Program (NEHRP) site condition B-C characterized by a shear wave velocity of 760 m/sec (2,493 ft/sec) in the uppermost 30 meters (~100 ft) of geologic material. It is noted that USGS 2008 seismic hazard maps are developed for the NEHRP B-C Boundary site condition (Petersen et al., 2008). Ground motion prediction equations by Spudich et al. (1999) and by Boore and Atkinson (2008) were used in this site-specific PSHA to estimate seismic ground motion response spectra in bedrock ranging from the B-C boundary condition to hard bedrock conditions. The selected attenuation models predict seismic ground motion amplitude scaling for earthquakes caused by normal slip on regional faults which is a tectonic characteristic of the intermountain west Basin and Range geologic province within which the site is situated.

The PSHA was performed using a logic-tree format in which a total of 4 seismic source models were convolved with three ground motion prediction models. This method produced 12 combinations of seismic source and ground motion models. The weighed PSHA results for these 12 examined cases are listed below.

Table-1 Uniform Hazard Response Spectra – Peak Horizontal Amplitudes in Bedrock

Annual Probability of Exceedance	Peak Horizontal Ground Acceleration	Spectral Acceleration (5% damping ratio)	Pseudo-Relative Velocity (5% damping)
2.1×10^{-3}	44.69 cm/sec^2 0.046 g	119.92 cm/sec^2 (5 Hz) 0.122 g	5.21 cm/sec (2.5 Hz) 2.05 in/sec (2.5 Hz)
10^{-3}	61.37 cm/sec^2 0.063 g	161.15 cm/sec^2 (5 Hz) 0.164 g	6.96 cm/sec (2.5 Hz) 2.74 in/sec (2.5 Hz)
10^{-4}	147.09 cm/sec^2 0.150 g	373.09 cm/sec^2 (5 Hz) 0.381 g	15.97 cm/sec (2.5 Hz) 6.29 in/sec (2.5 Hz)
10^{-5}	293.61 cm/sec^2 0.299 g	743.50 cm/sec^2 (5 Hz) 0.758 g	33.53 cm/sec (1.0 Hz) 13.20 in/sec (1.0 Hz)

The site-specific ground motion amplitudes are less than those determined for the 2008 update of the USGS national hazard maps. USGS PGA estimates are 30% higher at 10^{-3} per year and 40% higher at 10^{-5} per year than values shown above determined in the site-specific PSHA. The difference in seismic hazard estimates can result from the following possible causes.

- The site-specific PSHA used ground motion models for normal slip fault mechanisms; the USGS possibly used various fault mechanisms, or unspecified fault mechanisms, which predict higher amplitude seismic ground motions.
- The weighted result for the site-specific PSHA includes hazard results for hard bedrock attenuation models, which leads to lower amplitude seismic ground motions. The USGS 2008 results are for the NEHRP B-C Boundary site condition which is a firm bedrock condition that results in higher amplitude seismic ground motions relative to hard bedrock site conditions.
- The site-specific PSHA used a local earthquake frequency model determined for the ESRP; the USGS possibly used a larger background seismicity model for the Basin and Range province and a local cell earthquake activity rate that could exceed the historical earthquake rate (Petersen et al., 2008).

2.0 Regional Geology and Tectonics

Geologic Overview

The Eagle Rock Enrichment Facility (EREF) site lies within the Snake River Plain volcanic field of southeast Idaho approximately 32 km (20 mi) west of Idaho Falls, ID. Location of the site within the Snake River Plain (SRP) and locations of regional physiographic features are shown on **Figure 1**. The Snake River Plain is an arc shaped (convex south) belt of topographically subdued volcanic and sedimentary rocks. The SRP crosses southern Idaho, transecting the high-relief mountain ranges of the surrounding Basin and Range province. Volcanic and sedimentary rocks of the SRP occur in a 50 km to 100 km (31 mi to 62 mi) wide belt, spanning 600 km (373 mi) (Kuntz, 1979) from the Oregon-Idaho border, and northeastward to the Yellowstone Plateau. The total area of the SRP is about 40,400 km^2 (15,600 mi^2) (**Figure 1**). The SRP slopes upward from an elevation of about 750 m (2,500 ft) at the Oregon border to more than 1,500 m (5,000 ft) at Ashton, Idaho located northeast of the proposed site. The SRP is a relatively recent geologic feature that is superimposed on older and semi-contemporaneous geologic features of the Cordilleran Mountain Belt of western North America. Early volcanism of the SRP involved violent, voluminous eruptions of silicic rhyolite tuffs and lava flows, many of them associated with volcanic centers known as calderas. The nature of the volcanic activity changed over time to less violent, relatively lower volume eruptions of predominantly basaltic lavas. The older calderas and associated rhyolitic materials were buried beneath younger basaltic volcanic and sedimentary deposits.

Geologists have divided the Snake River Plain into eastern (ESRP) and western (WSRP) segments, based on physiographic features described above and tectonic characteristics. The EREF site is located close to the center of the ESRP, near the southeastern corner of the Idaho National Laboratory (INL). The ESRP has been structurally and volcanically active since approximately 17 million years ago (Ma) when this portion of the North American Plate began passing over a feature known as the Yellowstone hotspot. Radiometric age dating (Armstrong, et. al., 1975) indicates that the early silicic volcanism of the SRP becomes systematically younger from southwest to northeast. The northeastward progression of age dates supports the interpretation that the older silicic volcanic rocks of WSRP in southwest Idaho (Idavada volcanics and older rhyolites) and the younger silicic rocks of the ESRP in southeast Idaho (Heise volcanics) represent the track of a mantle plume (Pierce and Morgan, 1992) hotspot. The ESRP topographic depression resulted from subsidence behind the Yellowstone hotspot as it tracked towards its present location in northwest Wyoming (Hughes et al., 1999).

The igneous, metamorphic, and sedimentary rocks exposed in the mountainous areas adjacent to the ESRP range in age from Precambrian to Holocene. A geologic time scale is shown on **Figure 2**. Given their ages and position within the Central Cordillera of North America, these rocks have a highly varied yet common geological heritage that is tied to the development of western North America. Precambrian, Paleozoic, Mesozoic, and Early Cenozoic sedimentary formations were deposited along the western North American continent during several episodes of mountain building and erosion. Deformation of the Cordillera culminated during the Early Cenozoic with the formation of the easternmost thrust faults that can be observed in the Caribou and Snake River Ranges, East of Idaho Falls. Volcanic and intrusive igneous rocks were extruded/emplaced during and after the destruction

of the continental margin basins and are exposed in the Challis Volcanic Field and Idaho Batholith, Owyhee Plateau (north and west of the ESRP), and in the Basin and Range fault block mountains that generally surround the ESRP. The Basin and Range, fault block mountains formed in response to crustal extension during the Late Cenozoic.

The following sections provide general descriptions of the regional and local geology in the vicinity of the EREF site.

2.1 Regional Geology

Idaho-Wyoming Thrust Belt

The ESRP is bounded to the east by a physiographic region known as the Idaho-Wyoming Thrust Belt. The rocks and associated thrust faults of this region were the culmination of sedimentary deposition and deformation along the western margin of North America. Approximately 11,000 m (36,089 ft) of Paleozoic and Mesozoic sedimentary rocks were deposited near the shelf- basin boundary which ran the length of the North American craton (Monley, 1971; Blackstone, 1977).

Destruction of the continental margin began in late Jurassic moved eastward, and culminated in the east during Early Eocene time (Armstrong and Oriel, 1965). Structural features associated with the Idaho-Wyoming Thrust Belt include low-angle thrust faults and folds. Armstrong and Oriel (1965) determined the stratigraphic throw of the thrusts to be near 6100 m (20,013 ft) and lateral displacements near 16 km and 25 km (9.9 mi and 15.5 mi). Younger tectonic features of the Basin and Range and SRP have been superimposed on the Thrust Belt.

Idaho Batholith

The Idaho Batholith is a large region of multiple granitic plutons covering over 38,850 km^2 (15,000 mi^2) in central portions of Idaho. The batholith formed during two stages of activity in the Cretaceous Period, 105 to 75 Ma, and 85 to 65 Ma. The batholith formed beneath the surface as the Cretaceous oceanic Farallon Plate was subducted beneath the North American Plate (Hyndman, 1983). The southern portion of the Idaho Batholith is known as the Atlanta Lobe and it occurs north of the western end of the ESRP. As the plutons of the Idaho Batholith were emplaced, the older overlying rocks decoupled along low angle faults and moved laterally away from the uplifted area (Hyndman, 1983)

Challis Volcanic Field

The Challis volcanic field is an area of volcanism dating from approximately 34 to 56 Ma northwest of the ESRP. Three stages of eruptive activity occurred during this time (Sanford, 2005). The first stage was the eruption of andesite and dacite lava flows. Up to 1,524 m (5,000 ft) of andesitic and dacite volcanic deposits cover the area. The second eruption stage consisted of explosive ash-flow tuff

eruptions of rhyolite and dacite from calderas. The last stage was the formation of dacite dome complexes. Basin and Range extension caused faulting in the area (Sanford, 2005).

Owyhee Plateau

The Owyhee Plateau is an area of volcanic rocks located southwest of the ESRP. Volcanic activity in this area began approximately 17.5 Ma near the intersection of the Oregon-Idaho-Nevada borders, as the North American Plate passed over the Yellowstone (hotspot) mantle plume (Shoemaker and Hart, 2002). Initial activity was synchronous with flood basalts that were erupted onto the Columbia and Oregon Plateaus. Younger silicic volcanism in this area is related to large cataclysmic eruptive centers (Shoemaker and Hart, 2002).

Basin and Range

Extensional tectonism in the Basin and Range began around 30 Ma in present day Nevada (Kuntz, 1979). In Idaho, physiographic features that are typical of the Basin and Range province can be found north and south of the ESRP. Folded and thrust faulted Paleozoic and Mesozoic rocks that have been affected by extensional tectonics are found throughout the Idaho portion of the Basin and Range province (Kuntz and Dalrymple, 1979). Reactivation of Late Mesozoic and Early Cenozoic thrust fault surfaces, and normal faulting occurred during Tertiary and Quaternary time, uplifting the block faulted mountain ranges (Link and Janecke, 1999). Movement along range front normal faults has been observed throughout the province as crustal extension continues. The Lost River Range, Lemhi Range, and Beaverhead Range are three mountain ranges that developed along Basin and Range structures located north-northwest of the EREF site area. The tectonic setting of these areas and their apparent relationship with the ESRP volcanic rift zones will be discussed later in this section.

Western Snake River Plain

The Western Snake River Plain (WSRP) is a large structural graben that formed between 10 and 12 Ma (Shervais et al., 2005) and is filled with sediments and basalts. Extensive rhyolite deposits were extruded coincident within and adjacent to the WSRP graben (Shervais, et al, 2005). Rhyolitic volcanic activity in the WSRP occurred between 11.8 to 9.2 Ma as the North American Plate passed over the Yellowstone hotspot mantle plume. Basaltic lava flow eruptions occurred between 9.0 and 7.0 Ma, and are interspersed within the graben with Miocene sediments (Vetter et al, 2005). A later phase of basaltic activity, shield volcanoes and cinder cones, began approximately 2.2 Ma and continued until approximately 0.7 Ma. The later basaltic volcanic deposits are also intermitted with fluvial and lacustrine sediments (Vetter et al., 2005). West of Twin Falls, the Snake River has cut a valley through the tertiary basin fill sediments and interbedded volcanic rocks. The stream drainage is well developed, except in areas covered by recent thin basalt flows.

Yellowstone Plateau

The Yellowstone Plateau is an area of contemporary seismicity, hydrothermal activity and recent volcanism in northeastern Idaho, southwestern Montana, and northwestern Wyoming.

Volcanic activity in this plateau occurred during three eruptive cycles (Christiansen and Hutchinson, 1987). Initial activity for each cycle began as small scale bimodal basaltic and rhyolitic eruptions. Rhyolitic eruptions are believed to have continued for several hundred thousand years during each eruptive cycle as the magma chamber continued to grow beneath the plateau. Each cycle ended in a large cataclysmic explosive eruption that dispersed ejecta hundreds of miles away from the Plateau. The three large caldera-forming eruptions that occurred at the end of each eruptive cycle were approximately 700,000 years apart, 2.0, 1.3, and 0.6 Ma (Christiansen and Hutchinson, 1987). The middle eruptive phase was associated with feature known as the Island Park Caldera near West Yellowstone, Montana and forms the northeastern boundary of the ESRP (Christiansen and Hutchinson, 1987). The mantle plume hotspot responsible for the formation of the SRP is now considered to underlie the Yellowstone Plateau, accounting for the geothermal features and the more than 6,000 km^3 (1,439 mi^3) of late Pliocene and Quaternary silicic volcanic rocks in the Yellowstone Plateau Volcanic Field (Christiansen, 2000). Hydrothermal activity at Yellowstone in the form of geysers, fumaroles, hot springs, and mud pots are present today.

Sedimentary Deposition

During the late Pleistocene, the geomorphology of the ESRP was affected by continued eruptions of basaltic lava flows and also by glaciation particularly in the mountains on the northern side of the ESRP (Hughes, 1999). Important processes associated with glaciation were outburst flooding that deposited gravels and granitic boulders on top of the basaltic lavas in the ESRP and drainages eroded into the basaltic lavas. Extensive eolian (wind) erosion of glacial silts and sands resulted in deposition of loess of variable thicknesses throughout the ESRP. Lacustrine deposits from the formation of pluvial lakes and ponds are found in some areas of the ESRP. In recent times, range fires, subsequent wind erosion and re-deposition of soils and sands have been the dominant processes affecting the surface of the ESRP (Hughes, 1999).

Eastern Snake River Plain

The Eastern Snake River Plain (ESRP) is an east-northeast trending topographic depression that extends approximately 100 km (62.1 mi) by 300 km (186.4 mi) through southeastern Idaho (Kuntz, 1979). Most of the ESRP has a gently rolling topography at elevations from about 1,830 m (6,000 ft) above sea level in the northeastern portion to about 1,070 m (3,500 ft) at the southeastern edge along the Snake River. Several prominent buttes are scattered along the central part of the ESRP, including Big Southern Butte, Middle Butte, East Butte, and Menan Buttes (**Figure 3**). Big Southern Butte is the largest, rising 760 m (2,493 ft) above the plain. The topographic features of the ESRP are of volcanic origin and may be associated with geologic structures that are oriented both perpendicular and parallel to its axis. The general trends of structures in the adjacent Basin and Range province are also perpendicular to the ESRP axis and fault block mountain ranges occur to the north, east, and south as shown on **Figure 1**. The northwest trends of many ESRP volcanic features and structures in the adjacent Basin and Range mountain ranges are similar because they are extensional tectonic features that developed within the same regional stress field. To the northeast and west, the ESRP is bounded by the Yellowstone and Owyhee Volcanic Plateaus, respectively.

The well preserved volcanic features and associated deposits of the ESRP have been the subject of numerous studies and technical papers. Additionally, many of the ESRP studies have been associated with the Idaho National Laboratory (INL) property located immediately northwest of the EREF site. Many of the published sources which are cited in this section are part of the geologic literature associated with the INL. The geologic history of the ESRP is dominated by late Tertiary to Quaternary events that deposited a thick sequence of volcanic rocks of rhyolitic and basaltic composition. The general order of major geologic events from early to most recent is as follows (Hughes, 1999):

1. Miocene to Pliocene age rhyolitic volcanism associated with Yellowstone mantle plume hotspot,
2. Miocene to Recent age crustal extension associated with the Basin and Range province,
3. Quaternary eruptions of basalts and associated buildup of elongated, intermingled lava fields, small shield volcanoes, and cinder cones,
4. Quaternary glaciation and associated eolian, fluvial, and lacustrine sedimentation.

The Yellowstone hotspot is considered to be responsible for formation of the ESRP. As the North American Plate passed over the Yellowstone hotspot beginning approximately 17 Ma, melting above the hotspot produced (Pierce and Morgan, 1992; Smith, 2004) thick rhyolitic ash flows, tuffs, and lavas. The hot spot has left a trail of volcanism that records the southwestward relative motion of the North American plate over a fixed mantle plume, at a rate of about 3 cm (1.2 in) per year.

Miocene and Pliocene rhyolitic calderas are believed to be buried under younger Pleistocene volcanic deposits. Subsidence within the ESRP began approximately 4 Ma, as the hotspot track continued to the northeast beneath and relative to the North American plate, to its present day location in northwest Wyoming. Cooling of the crust, crustal extension, increased loads from denser magmatic rocks, and isostatic adjustment were other factors contributing to subsidence. Approximately 1.5 km -2 km (0.9 mi – 1.2 mi) of subsidence has occurred within the ESRP and continues today as the crust continues to reach isostatic equilibrium (Smith, 2004).

Thermal contraction and subsidence in the ESRP occurred after the cessation of rhyolitic activity from the Yellowstone mantle plume (Christiansen and Embree, 1987a). The effects of the Yellowstone mantle plume persist to the present day and the heat flux (~110 mW/m^2) beneath the ESRP is the highest found in the region. Recent volcanic activity has been the greatest beneath the northeastern ESRP where most of the heat is concentrated (Smith, 2004). Tectonic processes, including uplift of the Yellowstone plateau above the mantle hotspot and normal faulting in the adjacent Basin and Range Province, maintain the high elevations and mountainous character of the region surrounding the ESRP.

At the land surface, Quaternary basaltic lava flows, monogenetic shield volcanoes, rhyolite domes, and accumulations of unconsolidated sediments of variable thickness dominate the regional physiography (Hughes et al., 1999). Scoria cones, pyroclastic deposits near the volcanic vents, dikes, and less chemically evolved basaltic rocks are found to a lesser extent within the ESRP (Hughes et al., 1999) than in the WSRP. Most of the surface (Kuntz et al., 1994) and subsurface basalt lava flows

(Champion et al., 2002) of the INL area have normal magnetic polarity associated with the Brunhes Normal Polarity Chron, and are therefore younger than 780 ka.

The distinctive low relief produced by coalesced shield and lava flows of the ESRP prompted Greeley (1982) to name the features of the area "basaltic plains volcanism." Basaltic plains volcanism of the ESRP involves a large number of small eruptive centers with comparatively low effusion rates (high frequency, low magnitude volcanism). It is estimated that approximately 3.3 km^3 (0.8 mi^3) per 1000 years of basaltic volcanic deposits erupted throughout the region during the past 15,000 years (Kuntz et al., 1992). Basaltic volcanism in the region occurred as lava and scoria was erupted from dikes beneath volcanic rift zones. The regional northwest trend of these zones and their associated vents suggest they were oriented perpendicular to the least-compressive regional stress.

The Volcanic features typically associated with the basaltic plains volcanism include:

- Low Profile Basaltic Shields (e.g. Kettle Butte) comprised of interlaced basaltic lava flows that are generally aligned along rifts or fissures (Hughes, 1999)
- Fissures, vents and flows associated with rift zones
- Lava tubes and channels that originate from both fissures in rift zones and less commonly in low shields

Over the last 13,000 years volcanism has occurred at seven monogenetic basaltic lava fields within the region. Locations of these lava fields near the site are shown on **Figure 3**.

- Shoshone
- Wapi
- Kings Bowl
- North Robbers
- South Robbers
- Cerro Grande
- Hells Half Acre

The Craters of the Moon volcanic field is compositionally and temporally different from the other lava fields listed above. It is a polygenetic volcanic field that evolved during several cycles of volcanism, consisting of numerous eruptive centers of basaltic through andesitic composition. Eruption ages at Craters of the Moon vents range from 1.5 to 15 ka (Kuntz, 1988).

Unlike the earlier silicic volcanism, no systematic, eastward migration of basaltic volcanism is apparent on the ESRP; and Holocene lavas (younger than 15,000 years) occur across the ESRP. No eruptions have occurred on the ESRP during recorded history, but the basaltic lava flows of the Hell's Half Acre lava field erupted near the southern boundary of the proposed site as recently as 5,400 years ago (Kuntz, 1986).

Axial Volcanic Zone

The axial volcanic zone is a northeast-trending, constructional volcanic highland that occupies the central topographic axis of the ESRP. It is underlain by many basalt lava flows erupted from many fissure eruptions and small shield volcanoes during the past 4 Ma. The proposed EREF site is situated within the axial volcanic zone.

Volcanic Rift Zones

Volcanic rift zones are found throughout the ESRP (**Figure 3**). Kuntz et al. (1992) suggest that as many as nine volcanic rift zones cross the ESRP. The majority of the rift zones reflect a northwest-southeast trending lineation similar to what is observed in the Basin and Range province to the north and south of the ESRP. The following volcanic rift zones (from northeast to southwest) are found in the ESRP (Kuntz et al., 1992):

- Spencer-High Point volcanic rift zone
- Menan volcanic rift zone
- Lava Ridge-Hells Half Acre volcanic rift zone
- Howe-East Butte volcanic rift zone
- Arco-Big Southern Butte volcanic rift zone
- The Great Rift volcanic rift zone
- Borkum volcanic rift zone
- Richfield-Burley Butte volcanic rift zone

The Rock Corral Butte volcanic rift zone is a southwest-northeast trending rift zone that is perpendicular to all other rift zones found in the ESRP. This rift zone is believed to be related to a Pre-tertiary zone of crustal weakness (Kuntz, 1979).

The northwest trending volcanic rift zones in the ESRP are believed to have formed within the same extensional, regional-stress field as the adjacent Basin and Range mountains. However, in contrast to the range front faults, there is evidence that the volcanic rift zones are underlain by basaltic dikes. The emplacement of magma as vertical dikes within the rift zones is believed to be the mechanism of crustal extension and low-magnitude seismicity within the ESRP volcanic province (Parsons and Thompson, 1991). Study of historical seismicity observed during dike intrusion events in analog regions of basaltic volcanism (Iceland, Hawaii, etc.) and the results of numerical and physical modeling indicate that dike intrusion beneath volcanic rift zones is capable of generating only small magnitude (M 3 – 5.5) earthquakes (Hackett, Jackson, and Smith, 1996). In contrast, crustal extension in of the surrounding Basin and Range occurs by normal faulting with accompanying earthquakes of varying magnitudes.

2.2 Eastern Snake River Plain Stratigraphy

Neogene silicic volcanic deposits of the Heise volcanic field, overlain by late Tertiary and Quaternary basalts and sediments of the Snake River Group, are the main geologic units beneath the EREF site in the ESRP. The Heise volcanics are mostly silicic lava flows and ash-flow tuffs, and are estimated to be greater than 1,000 m (3,280 ft) thick in some areas. The Snake River Group is composed of tholeiitic basalt lava flows, intercalated sedimentary deposits of lacustrine, alluvial and eolian origin, and minor silicic volcanic rocks.

3.0 Local Geology and Tectonics

3.1 Local Geology

The local geology of the area around the EREF site mainly consists of Late Tertiary basaltic volcanic rocks erupted during the last 500,000 yrs. Rhyolitic domes and alluvial fan deposits occur to a lesser extent within the region (Hughes et al., 1999). The site is located east of the Lava Ridge-Hells Half Acre rift zone. Volcanism and tectonic activity from this zone produced shield volcanoes, spatter cones, small calderas, and fissure eruptions (Hughes et al., 1999).

No volcanic rift zones or eruptive centers are observable at the EREF site and there are few notable geologic features within the proposed site boundaries (**Figure 4**). The most significant features include:

- All flows have the same general appearance of being highly vesicular, extensively jointed, and filled with cavities; and

- Several basalt flow outcrops exhibit a narrow linear morphology, suggestive of pressure ridges.

The site lies within a shallow topographic depression about 230 km^2 (88.8 mi^2) in area. This depression is bounded by surrounding topographically higher elevations ranging from 1,554 m to 1,585 m (5,098 ft – 5,200 ft). The summits of seven small basalt shield volcanoes rise above the surrounding terrain. Together, the gently sloping lava fields from these shield volcanoes (erupted mainly 200 - 400 ka) form a shallow topographic depression enclosing the proposed site. The local geology of the adjacent area surrounding the EREF site consists primarily of basaltic volcanic rocks that erupted during the last 500,000 yrs. Rhyolitic domes and alluvial fan deposits occur to a lesser extent within the adjacent region (Hughes et al., 1999).

Outside of the proposed site boundaries, the most significant geologic features include the following (**Figure 3**):

- *Axial Volcanic Zone*

Researchers have identified a northeast trending volcanic highland within the ESRP known as the axial volcanic zone (AVZ). The AVZ is a topographic high that runs parallel to the long axis of the ESRP (**Figure 3**). This zone of higher elevation is the locus of numerous volcanic features including lava flows, spatter cones, shield volcanoes, and rhyolitic domes. Volcanic activity within the AVZ has occurred in the last two million years. Additionally, a series of volcanic rifts and fissures are located perpendicular to the AVZ. The EREF site is located within the AVZ (**Figure 3**); however, no volcanic rifts or eruptive centers are located within the proposed site boundaries.

- *East, unnamed and Middle Buttes*:

East, unnamed, and Middle Buttes are located about 20 to 30 km (12 to 18 mi) from the western boundary, and East and Middle buttes stand well above the elevation of the ESRP. The age of these deposits range from 1.9 to 0.5 Ma (Kuntz and Dalrymple, 1979). East Butte is composed of parallel layers of rhyolitic lava (Kuntz and Dalrymple, 1979) with inclusions of basalt. The unnamed butte studied through well borings and outcrops is a rhyolitic dome (Kuntz and Dalrymple, 1979). Middle Butte has been less studied than East Butte thus less is known about its internal structure. The upper surface of Middle Butte is composed of approximately 75 m (246 ft) of basaltic lava flows, but an endogenous rhyolite dome is believed to underlie the butte at depth and to account for the uplift of the basalt lava flows (Kuntz and Dalrymple, 1979).

- *Lava Ridge – Hells Half Acre Rift Zone*

The Lava Ridge - Hells Half Acre rift zone (Kuntz et al., 1992) extends 50 km (31.1 mi) southeast across the ESRP from the southern end of the Lemhi Range and passes approximately 5 km (3.1 mi) west of the EREF site. The southeast end of the rift zone is defined by the dike-induced fissures and vent complex of the Hells Half Acre lava field. The central part of the rift zone is defined by several small- to medium-sized shield volcanoes with vents elongated north-south. The northwest end of the zone is ill defined by poorly exposed lava flows of reversed magnetic polarity, mantled by fluvial, lacustrine and eolian sediment. The earliest volcanism (>730 ka) occurred at the northwestern end, volcanism of the central part is of intermediate age (200-500 ka), and the youngest volcanism occurred about 5 ka at the Hells Half Acre lava field at the southeastern end of the zone.

.

- *Hells Half Acre Lava Field*

The EREF site is located approximately 0.5 km (1.1 mi) north, across Highway 20, from the northernmost outcrops of Hells Half Acre lava field (**Figure 3**). The volcanic features associated with this lava field consist of a basaltic shield volcano and its vents (Kuntz et al., 2002). The main basalt shield volcano and its eruptive-fissure system, is about 5 km (3.1 mi) south of the proposed site. Basaltic lavas at Hells Half Acre lava field were erupted along a fissure system and consist of 5.2-ka basaltic pahoehoe lavas. The vents of the shield volcano occur within an elongated area 800 m (2625 ft) long by 100-200 m (328 - 656 ft) wide (Kuntz et al., 2002). Lavas traveled more than 20 km southeast from their vents, forming a lava field composed of many individual flows up to 100 m (328 ft)

wide and over 10 m (33 ft) thick. Hells Half Acre lava flows cover approximately 400 km^2 (154.4 mi^2) and form one of the largest lava fields on the ESRP. Besides lava flows, spatter and cinder deposits are also found within the lava field and reflect the explosive nature the volcano at different times in its eruptive history. A northwest- trending tension crack is considered to be the feeder system for the fissure eruptions that controlled the lava field (Hughes et al., 1999).

- *Kettle Butte*

Kettle Butte, is located about 1.6 km (1 mi) off the northeastern corner of the site (**Figure 4**), and is one of the largest ESRP basalt shield volcanoes. Its prominent summit is occupied by several small collapse craters and pyroclastic cones. Eruptions of Kettle Butte produced an extensive lava field covering at least 320 km^2 (123.6 mi^2) and about 6 km^3 (1.4 mi^3) in volume (Kuntz and Dalrymple, 1979) (**Figure. 3**). Although the lava flowed mainly to the northeast, Kettle Butte is the source for most of the lava-flow outcrops within the boundaries of the proposed site. The normal magnetic polarity of Kettle Butte lava indicates an age of volcanism < 730 ka and the lava has a K-Ar age of 316 +/- 75 ka (sample 84ILe-1; Kuntz et al., 1994). The lava flows and near-vent pyroclastic deposits of Kettle Butte and most other basalt shield volcanoes near the proposed site are included as part of unit Qbc on the geologic map of the INL area, a widespread lithostratigraphic unit composed of middle Pleistocene basalt lava flows and minor pyroclastic deposits estimated to have erupted about 200 - 400 ka (Kuntz et al., 1994).

3.2 Local Stratigraphy

The stratigraphy of the EREF site was characterized by advancing a 223 m (732 ft) deep corehole near the geographic center of the proposed site. Geophysical logs were also obtained, including a subsurface photographic record of the inner borehole walls, a caliper log of borehole diameter, and a natural-gamma log. Visual examination of the core materials and selected geophysical logs were used to generally describe the subsurface lithologies, to identify individual basalt lava flows and sedimentary interbeds, to describe the overall stratigraphy of the borehole, and to suggest possible correlations of the GW-1 rock cores with other subsurface cores and outcrops near the drill site. Section 3.3 and Figure 3.3-17 of the EREF environmental report presents the results of GW-1 core examination.

Two types of materials were intersected: basalt lava flows (97.6%) and sedimentary interbeds (2.4%). No pyroclastic deposits were identified. About 59 individual lava flows were identified, ranging from < 0.61 m to 15.2 m (< 2 ft to 50 ft) in thickness. Based on preliminary reconnaissance observations at six roadside localities along a 12.9 km (8 mi) length of highway 20 to the south of the proposed site suggest the following tentative correlations between surface and subsurface lava flows. The three basalt lava flows in the uppermost 60 ft of GW-1, above the first sedimentary interbed, were erupted from Kettle Butte, a large shield volcano several kilometers east of the proposed site. Surface lava flows at the location of GW-1 are mapped as having erupted from Kettle Butte (Kuntz, et al., 1994), and subsurface basalt flows from the 1 m - 18 m (3 ft – 59 ft) interval of GW-1 are petrographically similar to surface outcrops of Kettle Butte lava flows on much of the proposed site.

Possible correlations of basalt flows intersected below 18 m (59 ft) in GW-1 are described in Section 3.4 of the EREF environmental report.

3.3 Regional and Local Tectonics

Extensional tectonics within the Basin and Range province, north and south of the ESRP, plays an important role in dike emplacement and local ESRP tectonics. Although it is believed that the shallow and mid-crustal magma chambers related to the Yellowstone hotspot have solidified and cooled, relatively high temperatures within the upper mantle beneath the ESRP continued to produce basaltic magmas that form dikes or have erupted onto the surface (Smith et al., 1996). Continued stretching of the ESRP in the northeast – southwest direction is evident by the northwest trending tension crack and fissure systems (Smith, 2004). Outside of the ESRP, the extension is accommodated by north to northwest-trending normal faulting (Parsons et al., 1998).

Three distinct structural features are common within the northern Basin and Range:

- Reactivated thrust faults – extension resulted in renewed movement along low angle, pre-Basin and Range structures
- Older Folds – deformation of originally flat lying rocks
- Normal faults –extensional stresses result in fault bounded bedrock masses that have been tilted and uplifted along segmented, listric normal faults; the faults are high angle near the land surface and intersect and/or curve into low-angle structures at depth

Thrust faults are associated with tectonic activity from the Mesozoic Cordilleran orogenic belt (Link and Janecke, 1999) and pre-Basin and Range extensionalism. However active normal fault grabens are believed to be linked to these older thrust fault and their preferential zones of weakness (Costenius, 1982). The Putnam thrust is an example of extensional normal faulting associated with a reactivated thrust fault located southeast of the ESRP (Kellogg et al., 1999). Extensional faulting within the Basin and Range province adjacent to the ESRP was initiated approximately 17 to 5 Ma (Rodgers and Anders, 1990; Janecke, 1992, 1993, 1994; Fritz and Sears, 1993; Anders et al., 1993; Sears and Fritz, 1998). To the north of the ESRP, the Lost River, Lemhi, and Beaverhead ranges show that the Basin and Range extension was accommodated by north to northwest trending normal faults.

Seismic activity in the Basin and Range is associated with rupture events, producing earthquakes, as faulting occurs. The 7.3 magnitude Borah Peak earthquake was a rupture event of the Lost River normal fault in 1983 (Link and Janecke, 1999). The Borah Peak earthquake produced an approximate 1.8 m (6 ft) dip slip. The Borah Peak earthquake was centered approximately 125 km (78 mi) from the EREF site. In contrast, emplacement and inflation of dikes has allowed the crust of the nearby ESRP to expand nearly aseismically by allowing release of accumulated elastic strain with only small magnitude earthquakes (Parsons et al., 1998).

Subsidence

Subsidence and volcanism have continued into recent times (Holocene). The ESRP has subsided approximately 1 km (0.6 mi) since the passage of the Yellowstone mantle plume beneath the area. The subsidence began approximately 4 Ma and continues today in response to isostatic adjustments to the mid-crustal intrusions of gabbro and crustal contraction as the area cools (Smith, 2004). The subsidence has not been uniform and regions with a faster subsidence have accumulated sediments at faster rates. Smith (2004) infers that a feature known as the Big Lost Trough, located along the north and northeastern boundary of the INL is an area of relatively higher subsidence, where up to 50% of the stratigraphic column is comprised of sedimentary interbeds within the basalt flow sequence.

Tension cracks, fissures, and faults

A tension crack is an extensional feature within the ESRP that forms as lava migrates beneath the surface in dikes. Tension cracks are commonly found together, up to five, with multiple crack sets found within a small area (Kuntz et al., 2002). These cracks are propagated as lava ascends to the surface at different rates and volumes. Tension cracks in the ESRP represent pressure cracks formed on the edges of fissures due to dike emplacement. Fissures represent the dikes that were able to breach the surface (Kuntz et al., 2002). Local tension cracks, faults, fissures, and grabens are found at Kings Bowl and Craters of the Moon lava fields, the Spencer-High Point and Arco-Big Southern Butte volcanic rift zones, and adjacent to the site in the Lava-Ridge – Hell's Half Acre volcanic rift zone (Kuntz et al., 2002) (**Figure 3**).

Kings Bowl and Craters of the Moon

Kings Bowl lava field erupted approximately 2,200 years ago (Kuntz et al., 2002). 18 eruptive fissure segments make up a 6.1 km (3.8 mi) fissure system which produced the volcanic materials and structures found here. Tension cracks at Kings Bowl extend to 11.3 km (7.0 mi) northwest-southeast. The Open Crack rift set at Craters of the Moon lava field are two tension cracks sets (Kuntz et al., 2002). At Minidoka, the northern tension crack set consists of two pairs of cracks which extend 8 km (5.0 mi) and 6.5 km (4.0 mi). The cracks are separated by 1.9 km (1.2 mi) and are 4,500 years old, the same age as the Craters of the Moon lava field. The New Butte crack system is a composite of two crack set segments. The northern and southern tension crack segments extend 5 km and 10 km (3.1 mi and 6.2 mi), respectively (Kuntz et al., 2002).

Spencer-High Point and Arco-Big Southern Butte

The Spencer – High Point rift zone is a west-northwest trending volcanic rift zone that extends ~70 km (43.5 mi). Vertical off-sets are observable associated with two grabens within the rift zone. The northern graben has steep walls up to 10 m (33 ft) high and is 700 m (2297 ft) wide by 1.4 km (0.9 mi) long. This graben is believed to be related to dike emplacement beneath the area (Kuntz et al., 2002) as evidenced by the eruptive fissures along the graben and volcanic vents. Similar to the northern graben the western graben has steep walls, up to 12 m (39 ft) high, is 2.5 km (1.6 mi) long and up to 250 m (820 ft) wide. Unlike the northern graben, the southern graben is believed to be related

to faulting in bedrock beneath the lava flows. This is based on a 14^{o} difference in the trend direction for southern graben (Kuntz et al., 2002).

The Arco-Big Southern Butte volcanic rift zone trends from the northwest to the southeast for ~45 km (28 mi). Extensional faults are abundant throughout Box Canyon, located at the north end of the Arco-Big Southern Butte rift zone. These faults have offsets ranging from 1 to 8 m (3.3 to 26.2 ft) and extend up to 4 km (2.5 mi) in length. The extensional faults mark a large graben ~10 km (6.2 mi) long and up to 3.5 km (2.2 mi) wide. Volcanic activity is absent within the northern portions of the graben but abundant on its flanks and in the southern region. This trend is due to faulting in the northwestern portion and dike emplacement within the central and southeastern portions (Kuntz et al., 2002).

Lava-Ridge – Hell's Half Acre

Tension cracks are evident within the Lava-Ridge - Hells Half Acre rift zone and lava field. Local tension cracks extend greater than 2 m (6.6 ft) in width. One individual tension crack found at Hells Half Acre lava field is approximately 1 km (0.6 mi) long (Kuntz et al., 2002). The total length of the measured tension cracks at Hell's Half Acre lava field is 4.3 km (2.7 mi). The total length of the fissure system at Hell's Half Acre is 5.5 km (3.4 mi).

Dike Emplacement

Dike emplacement and inflation are important controls on extension in the ESRP (Parsons et al., 1998). Dikes within the ESRP are believed to vertically ascend to the surface from depth (**Figure 5**). The vertical ascent of the dikes reduced the amount of faulting in the region. Instead an abundant amount of tension cracks and fissures are found (Kuntz et al., 2002). Parsons and Thompson (1991) found that in extensional basaltic systems normal faulting can be suppressed when magmatic pressures are greater than the least principle stress. These magmatic pressures push dikes against their walls effectively opposing tectonic stresses. Thus earthquakes and faulting are limited in areas with vertical dike emplacement, like the ESRP (Parsons and Thompson, 1991). Study of historical seismicity observed during dike intrusion events beneath volcanic rift zones in analog regions (Iceland, Hawaii, etc.), and the results of numerical and physical modeling of the dike intrusion process indicate that only small to moderate earthquakes (magnitude 3 - 5.5) are associated with dike intrusion (Parsons et al., 1998; Hackett and Smith, 1994; Hackett et al., 1996,). Parsons et al. (1998) estimated the rate of dike emplacement at 10 m (33 ft) (width) per 1,000 years at the estimated strain rate in the ESRP.

3.4 Conclusions on Geologic Setting

Tertiary volcanic activity has deposited over 1 km (0.6 mi) of basalt in the ESRP. This basalt overlies older calderas and associated rhyolitic deposits of the 10^{4} Ma caldera forming Yellowstone hotspot eruptions. Subsidence from the load removal of the Yellowstone mantle plume as it migrated to the northeast continues today (Smith, 2004). On a local scale, the EREF site is located between the

Circular Butte – Kettle Butte and Lava Ridge – Hell's Half Acre volcanic rift zones, and north of Hell's Half Acre lava field. The most recent volcanic activity in the area was at Hell's Half Acre approximately 4,100 years ago. Tension cracks and fissures found at Hell's Half Acre lava field are recognizable dike emplacement features (Kuntz et al., 2002). Dike emplacement rates within the ESRP are 10 m (33 ft) (width) per 1,000 years (Parsons et al., 1998). Subsidence, causing thinning and extensional tectonics in the ESRP, and high heat fluxes beneath the area allow for the continuation of dike emplacement (Smith, 2004). The northwest trending volcanic rift zones in the ESRP are generally parallel to several of the long axes of fault bounded mountain ranges of the adjacent Basin and Range Province. Both the mountain ranges and the volcanic rift zones are extensional tectonic features that developed in response to the same extensional, regional-stress field. However, in contrast to the range front faults, there is evidence that the volcanic rift zones are filled with basaltic magma from shallow mantle-upper crustal dikes. The emplacement of magma from dikes within the rift structures is believed to stabilize these features (Parsons and Thompson, 1991).

4.0 Regional Quaternary Faulting

The map of regional Quaternary Faults is illustrated on **Figure 7**. Distances to the site from the regional Quaternary Faults are annotated on **Figure 7** and listed below in **Table 2**. Information on Quaternary Faults was obtained from the USGS database (http://earthquake.usgs.gov/regional/qfaults/) and in Petersen et al. 2008, Documentation for the 2008 Update for the National Seismic Hazard Maps, USGS Open File Report 2008-1128.

Quaternary Faults are defined as having produced magnitude 6.0 or larger earthquakes during the past 1.6 million years from present. The USGS Quaternary Fault database includes approximately 300 faults in the inter-mountain West. Listed below are several faults that are most proximate to the EREF site and impacts of which are considered in the seismic hazard assessment.

Table 2 – Regional Quaternary Faults and Earthquake Activity Rates

USGS CODE	Name	a-value	b-value	M_{max}	Distance to site (km)	Comments
601	Lost River	1.8910	0.80	7	98 171	nearest branch to epicenter of Borah Peak 1983
602	Lemhi	2.007	0.80	7	60	nearest branch no M6 events
603	Beaverhead	1.704	0.80	7	105	nearest branch no M6 events
621	Island Park Caldera	--	--	--		Observed seismicity M < 3.0
726	Grand Valley	2.065	0.80	7.10	124	northern branch no seismicity
768	Teton	2.159	0.80	7.16	188	Observed seismicity M < 6.0
3501	Idaho Rift System	--	--	--	10	no seismicity, faulting is associated with Quaternary volcanic activity

5.0 Regional Seismic Activity

Seismic history of the site region (approximate 322 km (200 mi) radius) was compiled from regional and national databases including the ANSS catalog through June 2008 and the catalog of significant US earthquakes from 1568 to 1989. The majority of earthquakes in the regional and national catalogs are listed in the m_b magnitude scale. Catalog entries in the m_b magnitude scale are converted to the moment magnitude scale, M_W, using Equation 1 (Johnston, 1996). Ground motion models used in the PSHA predict spectral amplitudes using the M_W scale; therefore earthquake activity rates are determined relative to the M_W scale.

$$Mw = 3.45 - 0.473mb + 0.145mb^2 \qquad [1]$$

Figure 6 illustrates the regional seismicity map. A bounding block of 40.5^O to 46.5^O N Latitude and -116.5^O to -108.5^O W. Longitude is used to define the PSHA study region for the EREF site. This block encompasses a 322 km (200 mi) radius of the site.

The regional seismicity map illustrates the site being situated in a seismically inactive region of the eastern Snake River Plain (ESRP) and surrounded to the west, north, east and south by more seismically active zones in the Basin and Range tectonic province.

The most significant earthquakes include the following:

1. Hebgen Lake Earthquake Montana on August 18th 1959, Mw=7.7, 158 km (98 mi) NE of the site.
2. Borah Peak Earthquake Idaho on October 28th 1983, Mw=7.3, 125 km (78 mi) WNW of the site.
3. Shoshone Earthquake Idaho on November 11th 1905, M=5.3 – 5.7, 180 km (112 mi) WSW of the site.

The November 11, 1905 Shoshone earthquake is the largest earthquake reported for the eastern Snake River Plain within which the site is located. Due to the occurrence of this earthquake prior to seismograph monitoring in the region, the epicenter could be uncertain by 100 km (62 mi) or more [(Idaho National Laboratory at http://www.inl.gov/geosciences/earthquakes.shtml)]. The event could have an epicenter in the adjacent Basin and Range province that exhibits high rates of seismic activity than the ESRP. The 1905 earthquake, however, is analyzed in the PSHA as being associated with the ESRP.

Earthquakes of magnitude 5.0 and larger reported for the site region are listed in **Table 3**. Distances to the site are calculated for the 66 earthquakes listed in **Table 3**. The closest distance to the site of these larger regional earthquakes is about 112 km (70 mi).

Table 3 – Regional Earthquakes of Magnitude 5 and Larger

				-112.44	*43.5909*		MAG	Distance		Data	
Event #	Year	Month	Day	Longitude	Latitude	MAG	Type	Km	Mile	Source	Comments
1	1897	11	4	-112.600	45.300	6.40	FAMMT	190.1	118.1	USHIS	Mag from MMI area
2	1905	11	11	-114.500	42.900	5.70	M_L	183.4	113.9	USHIS	Shoshone EQ
3	1910	4	19	-112.500	46.000	5.40	M_L	267.5	166.2	USHIS	
4	1916	5	13	-116.500	44.200	5.30	M_L	331.7	206.1	USHIS	
5	1916	8	3	-116.500	41.500	5.60	M_L	405.0	251.7	USHIS	
6	1916	8	3	-116.500	41.500	5.80	M_L	405.0	251.7	USHIS	
7	1917	12	12	-111.300	43.000	5.30	M_L	113.1	70.3	USHIS	
8	1925	6	28	-111.240	46.400	6.75	M_L	325.7	202.4	USHIS	
9	1926	12	13	-111.200	46.100	5.40	M_L	295.1	183.4	USHIS	
10	1928	9	5	-115.200	42.100	5.20	M_L	279.0	173.3	USHIS	
11	1929	2	16	-111.300	46.100	5.60	M_L	292.6	181.8	USHIS	
12	1934	3	12	-112.800	41.700	6.60	M_L	211.9	131.7	USHIS	
13	1934	3	12	-112.500	41.500	5.10	M_L	232.1	144.2	USHIS	
14	1934	3	12	-112.500	41.500	6.00	M_L	232.1	144.2	USHIS	
15	1934	3	15	-112.500	41.500	5.10	M_L	232.1	144.2	USHIS	
16	1934	4	7	-111.500	41.500	5.50	M_L	244.5	151.9	USHIS	
17	1934	4	14	-112.500	41.500	5.25	M_L	232.1	144.2	USHIS	
18	1934	5	6	-113.000	41.500	5.50	M_L	236.6	147.0	USHIS	
19	1935	10	12	-112.000	46.600	5.90	M_L	335.8	208.6	USHIS	
20	1935	10	19	-112.000	46.600	6.25	M_L	335.8	208.6	USHIS	
21	1935	10	31	-112.000	46.600	6.00	M_L	335.8	208.6	USHIS	
22	1937	11	19	-113.900	42.100	5.40	M_L	203.7	126.6	USHIS	
23	1944	7	12	-115.060	44.410	6.10	M_L	228.1	141.7	USHIS	
24	1945	2	14	-115.090	44.610	6.00	M_L	239.6	148.9	USHIS	
25	1945	9	18	-116.500	40.600	5.10	M_L	471.1	292.7	USHIS	
26	1947	11	23	-111.710	44.820	6.25	M_L	148.3	92.1	USHIS	
27	1950	1	18	-110.500	40.500	5.30	M_L	378.5	235.2	USHIS	
28	1959	8	18	-111.210	44.710	7.70	M_W	158.2	98.3	USHIS	Hebgen Lake EQ
29	1959	8	18	-110.710	44.700	6.50	M_L	184.8	114.8	USHIS	
30	1959	8	18	-111.050	44.850	6.00	M_L	178.2	110.7	USHIS	
31	1959	8	18	-110.850	44.720	5.60	M_L	178.2	110.7	USHIS	
32	1959	8	18	-110.870	44.720	6.50	M_L	177.0	110.0	USHIS	
33	1959	8	19	-110.840	44.650	6.00	M_L	173.4	107.8	USHIS	
34	1962	8	30	-111.741	42.035	5.70	M_L	181.8	113.0	USHIS	
35	1962	8	30	-111.730	41.920	5.86	M_W	194.3	120.7	USHIS	

				-112.44	43.5909		MAG	Distance		Data	
Event #	Year	Month	Day	Longitude	Latitude	MAG	Type	Km	Mile	Source	Comments
36	1962	9	5	-112.089	40.715	5.20	M_L	320.5	199.1	USHIS	
37	1962	9	5	-112.090	40.720	5.20	m_b	320.0	198.8	ANSS	
38	1963	10	16	-114.800	44.300	5.90	m_b	204.4	127.0	ANSS	
39	1963	12	23	-114.700	44.300	5.10	m_b	197.0	122.4	ANSS	
40	1964	10	21	-111.600	44.800	5.80	m_b	149.9	93.2	ANSS	
41	1964	10	21	-111.810	44.730	5.80	m_b	136.0	84.5	ANSS	
42	1965	1	6	-112.700	44.900	5.10	m_b	146.8	91.2	ANSS	
43	1965	1	6	-112.750	44.770	5.10	m_b	133.2	82.8	ANSS	
44	1973	3	30	-110.333	44.298	5.07	m_b	185.8	115.4	ANSS	
45	1973	3	31	-110.491	44.513	5.10	m_b	186.1	115.7	ANSS	
46	1974	7	1	-111.089	44.564	5.10	m_b	152.6	94.8	ANSS	
47	1975	3	28	-112.525	42.063	6.00	m_b	169.8	105.5	ANSS	
48	1975	6	30	-110.604	44.688	6.10	m_b	190.3	118.3	ANSS	
49	1975	6	30	-110.718	44.766	5.30	m_b	189.2	117.6	ANSS	
50	1976	12	8	-110.790	44.760	5.50	m_b	184.6	114.7	ANSS	
51	1976	12	9	-110.807	44.756	5.10	m_b	183.3	113.9	ANSS	
52	1977	3	11	-111.500	44.848	5.20	m_b	158.3	98.4	ANSS	
53	1983	10	28	-113.857	44.058	7.30	M_W	124.8	77.5	ANSS	Borah Peak EQ
54	1983	10	28	-113.911	44.073	5.40	m_b	129.4	80.4	ANSS	
55	1983	10	29	-114.105	44.231	5.40	m_b	150.9	93.8	ANSS	
56	1983	10	29	-114.115	44.281	5.50	m_b	154.2	95.8	ANSS	
57	1994	2	3	-110.976	42.762	5.40	m_b	150.0	93.2	ANSS	
58	1994	2	4	-111.026	42.709	5.20	m_b	150.6	93.6	ANSS	
59	1994	2	11	-110.995	42.764	5.30	m_b	148.7	92.4	ANSS	
60	1994	4	7	-111.032	42.561	5.20	m_b	161.6	100.4	ANSS	
61	1994	6	7	-114.071	44.410	5.10	m_b	158.8	98.7	ANSS	
62	1995	2	3	-109.805	41.527	5.20	m_b	314.4	195.4	ANSS	
63	1995	8	28	-110.307	44.119	5.10	m_b	180.5	112.2	ANSS	
64	1999	8	20	-112.793	44.793	5.10	m_b	136.4	84.7	ANSS	
65	2001	4	21	-111.395	42.925	5.30	m_b	112.2	69.7	ANSS	
66	2005	7	26	-112.615	45.345	5.60	m_b	195.2	121.3	ANSS	

6.0 Regional Seismic Source Zones

Regional seismic source zones surrounding the EREF site employed by Petersen et al. (2008) for the 2008 update of the National Seismic Hazard Maps are illustrated on **Figure 8**. This USGS 2008 seismic source zonation is applied as Model 1 for the site-specific PSHA for the EREF site. The two regional seismic sources include the eastern Snake River Plain and the Yellowstone Parabola. The site is centrally located in the northeastern end of the ESRP. Nearest distances from the site to boundaries with the surrounding Yellowstone Parabola zone are 54 km (34 mi) (west), 65 km (40 mi) (east), and 180 km (112 mi) (northeast).

Model 1 is applied in two versions. The first version assigns a uniform earthquake activity rate to the entire area of the Yellowstone Parabola source zone. The second version assigns localized earthquake activity rates to three segments of the Yellowstone Parabola, the western segment, northern segment, and eastern segment, to address differences in observed seismic activity within the large Yellowstone Parabola seismic source zone.

Figure 9 illustrates seismic source zone Model 2 which includes five regional seismic sources defined on the basis of higher spatial densities of historical earthquake epicenters. The Yellowstone Parabola zone is differentiated into 5 seismic sources. The Eastern Snake River Plain zone containing the site is also used in Model 2. Differences in spatial coverage of the five regional seismic sources and the Yellowstone Parabola are shown on **Figure 9**.

The third seismic source model, Model 3, is illustrated on **Figure 10**. Model 3 uses the Eastern Snake River Plain and the five regional seismic sources that subdivide the Yellowstone Parabola source with the addition of 5 Quaternary Faults (Q 601, Q602, Q603, Q726 and Q 768) listed in **Table 2**. The Idaho Rift System faults (Q3501) are not included due to seismic inactivity and no recurrence models included in Petersen et al. (2008).

Table 4 provides earthquake activity rates determined for the regional seismic source zones in Models 1 through 3. Listed are the recurrence model parameters (a-value, b-value), annual rates of earthquakes of magnitude 5.0 M_W and larger, and maximum magnitude, M_W, in each seismic source zone or Quaternary Fault.

Table 4 – Seismicity Parameters for Regional Seismic Sources and Quaternary Faults

Model	Seismic Zone	a-value	b-value	Rate M_W 5 and Larger	M_{max}	Comments
1, 2, 3	Eastern Snake River Plain	2.931	0.945	0.0160	7.0	Shoshone Eq M=5.3 - 5.7
1 U	Yellowstone Parabola	4.227	0.940	0.3365	7.7	Hebgen Lake M=7.7
1 L	Yellowstone Parabola west segment	3.065	0.830	0.0822	7.7	Borah Peak M=7.3
1 L	Yellowstone Parabola north segment	3.092	0.831	0.0865	7.7	Hebgen Lake M=7.7
1 L	Yellowstone Parabola east segment	5.437	1.366	0.0458	7.7	March 28, 1975 M=6.0
2, 3	Lost River – Lemhi Zone	2.871	0.801	0.0735	7.7	Borah Peak M=7.3
2, 3	Southwest Montana	4.369	1.134	0.0500	7.7	June 28, 1925 M=6.75
2, 3	Yellowstone Zone	2.902	0.815	0.0671	7.7	Hebgen Lake M=7.7
2, 3	Tetons Zone	5.258	1.364	0.0274	7.7	Feb. 3, 1994 M=5.4
2, 3	Northern Utah Zone	3.66	1.011	0.0403	7.7	March 12, 1934 M=6.6
3	601 – Lost River Fault	1.891	0.80	.0078	7.3	Borah Peak M=7.3 in 1983
3	602 – Lemhi Fault	2.007	0.80	.0102	7.0	
3	603 – Beaverhead Fault	1.704	0.80	.0051	7.0	
3	726 – Grand Valley Fault	2.065	0.80	.0116	7.1	
3	768 – Teton Fault	2.159	0.80	.0144	7.2	

7.0 Ground Motion Models

Ground motion prediction equations were selected for the PSHA for the EREF site on the basis of the following criteria.

- Predict ground motion for slip on normal faults.
- Predict spectral velocity or spectral acceleration for a range of ground motion frequencies.
- Recent publications using a large and current strong motion database.
- Predict ground motion for bedrock site conditions.

Two attenuation models meeting the above criteria were selected. These include Spudich et al. (1999) and Boore and Atkinson (2008).

Following is a summary of these models. Journal publications for these two attenuation models are provided in Appendix A.

Ground Motion Model	Description
Spudich et al. (1999) **SEA99** BSSA Vol. 89, No. 5 Oct. 1999, pp. 1156-1170.	Revision to Spudich et al. (1996) SEA96 Prediction for extensional tectonic regimes, e.g. normal slip on faults Scaling to moment magnitude, M_W Predictions of peak ground acceleration (PGA) and pseudo-relative velocity (PSRV) (5% damping) for periods of 0.10 to 2.0 sec Predictions for bedrock (Vs 620 m/sec (2,034 ft/sec) and greater)
Boore and Atkinson (2008) **B&A08** Earthquake Spectra, Vol. 24, No. 1, pp. 99-138	Derived in PEER Next Generation Attenuation Project Predictions for various fault types (unknown, reverse, normal, strike-slip) Scaling to moment magnitude, M_W Prediction of PGA, peak ground velocity (PGV) and spectral acceleration (SA) (5% damping) for periods of 0.01 to 10.0 sec Predictions for bedrock (V_{S30} range from 760 m/sec (2,493 ft/sec) to 1,300 m/sec (4,265 ft/sec)) V_{S30} represents the average shear wave velocity in the topmost 30 m (98 ft) of soil/rock column.

7.1 Spudich et al. (1999) Model - SEA99

The **SEA99** ground motion prediction equations (GMPE) are shown below. Equations are given on page 1162 of Spudich et al. (1999); the complete journal article is included in Appendix A.

The general forms of the regression equations for development of the GMPE are shown below in Equations 2 and 3.

$$log_{10}(Z) = b_1 + b_2(M-6) + b_3(M-6)^2 + b_5 log_{10} D + b_6 \Gamma \quad [2]$$

Where:

Z	is peak horizontal acceleration (g) or pseudo-velocity response (cm/sec) at 5% damping for the geometrical mean horizontal component
M	is Moment Magnitude
Γ	0 for a rock site, 1 for a soil site
b_1, $b_2 \ldots b_6$, and h	are regression coefficients that depend on period.

$$D = \sqrt{r_{jb}^2 + h^2} \quad [3]$$

Where:

r_{jb}	is Joyner-Boore distance, or closest horizontal distance to the projection of the fault plane.

Coefficients ($b_1 - b_6$, h) for the mean ground motion predictions and values of aleatory uncertainty (σ_1, σ_2, σ_3) are shown in the **Table 5** [i.e. Table 2 on page 1163 of Spudich et al. (1999)]. The **SEA99** ground motion model includes predictions at 46 closely spaced periods between 0.1 second and 2.0 seconds. Equation 4 shows computation of the standard deviation of $log_{10}(Z)$, the median ground motion estimate provided by Equation 2.

$$\sigma_{logZ} = \sqrt{\sigma_1^2 + \sigma_2^2} \quad [4]$$

Table 5 – Smoothed Coefficients for Regression Relation SEA99 for Geometric Mean PGA and 5% Damped PSV

Period (sec)	nr*	ne*	b_1	b_2	b_3	b_5	b_6	h (km)	σ_1	σ_2	σ_3
PGA	142	39	0.299	0.229	0.000	-1.052	0.112	7.270	0.172	0.108	0.094
0.100	131	38	2.144	0.327	-0.098	-1.250	0.064	9.990	0.205	0.181	0.110
0.110	132	38	2.155	0.318	-0.100	-1.207	0.064	9.840	0.205	0.168	0.111
0.120	132	38	2.165	0.313	-0.101	-1.173	0.065	9.690	0.204	0.156	0.113
0.130	132	38	2.174	0.309	-0.101	-1.145	0.067	9.540	0.205	0.146	0.114
0.140	132	38	2.183	0.307	-0.100	-1.122	0.069	9.390	0.205	0.137	0.115
0.150	132	38	2.191	0.305	-0.099	-1.103	0.072	9.250	0.205	0.129	0.116
0.160	132	38	2.199	0.305	-0.098	-1.088	0.075	9.120	0.206	0.122	0.117
0.170	132	38	2.206	0.305	-0.096	-1.075	0.078	8.990	0.207	0.116	0.118
0.180	132	38	2.212	0.306	-0.094	-1.064	0.081	8.860	0.208	0.110	0.119
0.190	132	38	2.218	0.308	-0.092	-1.055	0.085	8.740	0.209	0.105	0.119
0.200	132	38	2.224	0.309	-0.090	-1.047	0.088	8.630	0.210	0.100	0.120
0.220	132	38	2.234	0.313	-0.086	-1.036	0.095	8.410	0.212	0.092	0.121
0.240	132	38	2.242	0.318	-0.082	-1.029	0.102	8.220	0.214	0.086	0.122
0.260	132	38	2.250	0.323	-0.078	-1.024	0.108	8.040	0.216	0.081	0.123
0.280	132	38	2.257	0.329	-0.073	-1.021	0.115	7.870	0.218	0.076	0.124
0.300	132	38	2.263	0.334	-0.070	-1.020	0.121	7.720	0.220	0.073	0.125
0.320	132	38	2.268	0.340	-0.066	-1.019	0.126	7.580	0.221	0.070	0.126
0.340	132	38	2.272	0.345	-0.062	-1.020	0.132	7.450	0.223	0.067	0.126
0.360	132	38	2.276	0.350	-0.059	-1.021	0.137	7.330	0.225	0.065	0.127
0.380	132	38	2.279	0.356	-0.055	-1.023	0.142	7.220	0.227	0.064	0.128
0.400	132	38	2.282	0.361	-0.052	-1.025	0.147	7.110	0.228	0.063	0.128
0.420	132	38	2.285	0.365	-0.049	-1.027	0.151	7.020	0.230	0.062	0.129
0.440	132	38	2.287	0.370	-0.047	-1.030	0.155	6.930	0.231	0.061	0.129
0.460	132	38	2.289	0.375	-0.044	-1.032	0.159	6.850	0.233	0.061	0.129
0.480	132	38	2.291	0.379	-0.042	-1.035	0.163	6.770	0.234	0.060	0.130
0.500	132	38	2.292	0.384	-0.039	-1.038	0.166	6.700	0.235	0.061	0.130
0.550	132	38	2.294	0.394	-0.034	-1.044	0.174	6.550	0.238	0.061	0.131
0.600	132	38	2.295	0.403	-0.030	-1.051	0.181	6.420	0.241	0.063	0.132
0.650	132	38	2.295	0.411	-0.026	-1.057	0.187	6.320	0.243	0.065	0.132
0.700	132	38	2.294	0.418	-0.023	-1.062	0.192	6.230	0.245	0.068	0.133
0.750	132	38	2.292	0.425	-0.020	-1.067	0.197	6.170	0.247	0.071	0.133
0.800	132	38	2.290	0.431	-0.018	-1.071	0.200	6.110	0.249	0.074	0.134
0.850	131	38	2.287	0.437	-0.016	-1.075	0.203	6.070	0.250	0.077	0.134
0.900	131	38	2.284	0.442	-0.015	-1.078	0.206	6.040	0.251	0.081	0.134
0.950	131	38	2.280	0.446	-0.014	-1.081	0.208	6.020	0.253	0.085	0.135
1.000	131	38	2.276	0.450	-0.014	-1.083	0.210	6.010	0.254	0.089	0.135
1.100	119	35	2.267	0.457	-0.013	-1.085	0.213	6.010	0.255	0.097	0.135

Table 5 – (continued)

Period (sec)	nr*	ne*	*b1*	*b2*	*b3*	*b5*	*b6*	*h* (km)	σ1	σ2	σ3
1.200	116	35	2.258	0.462	-0.014	-1.086	0.214	6.030	0.257	0.106	0.136
1.300	116	35	2.248	0.466	-0.015	-1.085	0.214	6.070	0.258	0.115	0.136
1.400	114	34	2.237	0.469	-0.017	-1.083	0.213	6.130	0.258	0.123	0.136
1.500	114	34	2.226	0.471	-0.019	-1.079	0.212	6.210	0.259	0.132	0.137
1.600	114	34	2.215	0.472	-0.022	-1.075	0.210	6.290	0.259	0.141	0.137
1.700	105	34	2.203	0.473	-0.025	-1.070	0.207	6.390	0.259	0.150	0.137
1.800	105	34	2.192	0.472	-0.029	-1.063	0.204	6.490	0.259	0.158	0.137
1.900	105	34	2.180	0.472	-0.032	-1.056	0.201	6.600	0.258	0.167	0.137
2.000	105	34	2.168	0.471	-0.037	-1.049	0.197	6.710	0.258	0.175	0.137

Table 6 lists coefficients for PGA and PSRV at 5 periods used in the site-specific PSHA for the EREF site. The standard error, $\sigma_{log10(Z)}$, shown in **Table 6** was calculated using Equation 4.

Table 6 – Coefficients for SEA99 Ground Motion Prediction Equations

Param	Period	Frequency	b1	b2	b3	b5	b6	h	σ1	σ2	$\sigma_{log10(Z)}$
PGA	0.05	20.00	0.299	0.229	0.000	-1.052	0.112	7.270	0.172	0.108	0.203
PSRV	0.10	10.00	2.144	0.327	-0.098	-1.250	0.064	9.990	0.205	0.181	0.273
PSRV	0.20	5.00	2.224	0.309	-0.090	-1.047	0.088	8.630	0.210	0.100	0.233
PSRV	0.40	2.50	2.282	0.361	-0.052	-1.025	0.147	7.110	0.228	0.063	0.237
PSRV	1.00	1.00	2.276	0.450	-0.014	-1.083	0.210	6.010	0.254	0.089	0.269
PSRV	2.00	0.50	2.168	0.471	-0.037	-1.049	0.197	6.710	0.258	0.175	0.312

7.2 Boore and Atkinson (2008) Model – B&A08

The form of the **B&A08** ground motion prediction equation is shown below in Equation 5 (Boore and Atkinson, 2008, p. 106). The regression model adopted in **B&A08** includes separate terms for magnitude scaling, distance scaling, site amplification effects, and total aleatory uncertainty. Ground motion predictions are based on the moment magnitude scale, M_W.

$$\ln Y = F_M(M_W) + F_D(R_{JB}, M_W) + F_S(V_{S30}, R_{JB}, M_W) + \varepsilon\sigma_T \qquad [5]$$

Where:

$\ln Y$	Y is average horizontal component of peak ground acceleration (PGA), peak ground velocity (PGV) and peak spectral acceleration (PSA) for 5% damping, Y has units of (g) for PGA and PSA and units of cm/sec for PGV
F_M	is magnitude scaling
F_D	is distance scaling
F_S	is site amplification scaling
R_{JB}	is closest horizontal distance to the projection of the fault plane
V_{S30}	is average shear wave velocity (m/sec) from surface to a depth of 30 m (98 ft)
M_W	is Moment Magnitude
ε	is the fractional number of standard deviations away from the mean value, lnY
σ_T	$= \sqrt{\sigma^2 + \tau^2}$
σ	is intra-event aleatory uncertainty
τ	is inter-event aleatory uncertainty

Equations 6 and 7 define the **B&A08** magnitude scaling parameter, F_M.

a) $M \leq M_h$

$$F_M(M_W) = e_1U + e_2SS + e_3NS + e_4RS + e_5(M_W-M_h) + e_6(M_W-M_h)^2 \quad [6]$$

b) $M > M_h$

$$F_M(M_W) = e_1U + e_2SS + e_3NS + e_4RS + e_7(M_W-M_h) \quad [7]$$

Where:	$F_M(M_W)$	is the magnitude scaling parameter in Equation 5
	U	is unspecified fault type, =1 if true, 0 if false
	SS	is strike-slip fault type, =1 if true, 0 if false
	NS	is normal slip fault type, =1 if true, 0 if false
	RS	is reverse slip fault type, =1 if true, 0 if false
	M_h	is hinge magnitude for shape of the magnitude scaling
	M_W	is Moment Magnitude
	$e_1..e_7$	are regression coefficients

Equation 8 defines the **B&A08** magnitude scaling parameter, F_D.

$$F_D(R_{JB},M_W) = [c_1 + c_2(M_W - M_{ref}]\ln(R/R_{ref}) + c3(R-R_{ref}) \quad [8]$$

Where:

F_D	is the distance scaling parameter in Equation 5
R	$= \sqrt{R_{JB}^2 + h^2}$
M_W	is Moment Magnitude
$c_1..c_3$	are regression coefficients
M_{ref}	is a regression coefficient
R_{ref}	is a regression coefficient

Equation 9 defines the **B&A08** site amplification parameter, F_S, in terms of linear, F_{LIN}, and non-linear, F_{NL}, terms.

$$F_S = F_{LIN} + F_{NL} \quad [9]$$

The linear term is defined in Equation 10. Only the linear term, Equation 10, was used in the seismic hazard assessment for the EREF site due to the bedrock site condition.

$$F_{LIN} = b_{lin}\ln(V_{S30}/V_{ref}) \quad [10]$$

Where:

F_S	is the site amplification parameter in Equation 5
V_{S30}	is the average shear wave velocity from ground surface down to a depth of 30 m (98 ft)
V_{ref}	is the reference velocity of 760 m/sec (2,493 ft/sec) corresponding to NEHRP B-C boundary site condition
b_{lin}	is a period dependent regression coefficients

Boore and Atkinson (2008) provide equations to predict peak ground acceleration (PGA), peak ground velocity (PGV), and spectral acceleration SA (5% damping) at 21 periods between 0.01 second and 10 seconds. **Table 7** lists coefficients for parameter F_{LIN} in the **B&A08** model. Predictions for PGA and SA at 9 periods were used in the PSHA for the EREF site; these are shown in bold type in **Table 7**. SA equations were selected for periods also defined in the **SEA99** ground motion model.

Table 7 – Coefficients for Boore & Atkinson (2008) Ground Motion Prediction Equations for Parameter F_{LIN}

	b_{lin}	b_1	b_2
PGV	-0.600	-0.500	-0.060
PGA	**-0.360**	**-0.640**	**-0.140**
Period (sec)	**Spectral Acceleration 5% damping**		
0.010	**-0.360**	**-0.640**	**-0.140**
0.020	-0.340	-0.630	-0.120
0.030	-0.330	-0.620	-0.110
0.050	**-0.290**	**-0.640**	**-0.110**
0.075	-0.230	-0.640	-0.110
0.100	**-0.250**	**-0.600**	**-0.130**
0.150	-0.280	-0.530	-0.180
0.200	**-0.310**	**-0.520**	**-0.190**
0.250	-0.390	-0.520	-0.160
0.300	-0.440	-0.520	-0.140
0.400	**-0.500**	**-0.510**	**-0.100**
0.500	-0.600	-0.500	-0.060
0.750	-0.690	-0.470	0.000
1.000	**-0.700**	**-0.440**	**0.000**
1.500	-0.720	-0.400	0.000
2.000	**-0.730**	**-0.380**	**0.000**
3.000	-0.740	-0.340	0.000
4.000	-0.750	-0.310	0.000
5.000	**-0.750**	**-0.291**	**0.000**
7.500	-0.692	-0.247	0.000
10.000	**-0.650**	**-0.215**	**0.000**

Coefficients for **B&A08** parameter F_D are listed in **Table 8**. Periods selected for the PSHA for the EREF site are listed in bold type.

Table 8 – Coefficients for Boore & Atkinson (2008) Ground Motion Prediction Equations for Parameter F_D

	c_1	c_2	c_3	h
PGV	-0.87370	0.10060	-0.00334	2.54
PGA	**-0.66050**	**0.11970**	**-0.01151**	**1.35**
Period (sec)	**Spectral Acceleration 5% damping**			
0.010	**-0.66220**	**0.12000**	**-0.01151**	**1.35**
0.020	-0.66600	0.12280	-0.01151	1.35
0.030	-0.69010	0.12830	-0.01151	1.35
0.050	**-0.71700**	**0.13170**	**-0.01151**	**1.35**
0.075	-0.72050	0.12370	-0.01151	1.55
0.100	**-0.70810**	**0.11170**	**-0.01151**	**1.68**
0.150	-0.69610	0.09884	-0.01113	1.86
0.200	**-0.58300**	**0.04273**	**-0.00952**	**1.98**
0.250	-0.57260	0.02977	-0.00837	2.07
0.300	-0.55430	0.01955	-0.00750	2.14
0.400	**-0.64430**	**0.04394**	**-0.00626**	**2.24**
0.500	-0.69140	0.06080	-0.00540	2.32
0.750	-0.74080	0.07518	-0.00409	2.46
1.000	**-0.81830**	**0.10270**	**-0.00334**	**2.54**
1.500	-0.83030	0.09793	-0.00255	2.66
2.000	**-0.82850**	**0.09432**	**-0.00217**	**2.73**
3.000	-0.78440	0.07282	-0.00191	2.83
4.000	-0.68540	0.03758	-0.00191	2.89
5.000	**-0.50960**	**-0.02391**	**-0.00191**	**2.93**
7.500	-0.37240	-0.06568	-0.00191	3.00
10.000	**-0.09824**	**-0.13800**	**-0.00191**	**3.04**

Coefficients for **B&A08** parameter F_M are listed in **Table 9**. Periods selected for the site-specific PSHA for the EREF site are listed in bold type.

Table 9 – Coefficients for Boore & Atkinson (2008) Ground Motion Prediction Equations for Parameter F_M

	e_1	e_2	e_3	e_4	e_5	e_6	e_7	M_h
PGV	5.00121	5.04727	4.63188	5.08210	0.18322	-0.12736	0.00000	8.50
PGA	**-0.53804**	**-0.50350**	**-0.75472**	**-0.50970**	**0.28805**	**-0.10164**	**0.00000**	**6.75**
Period (sec)	**Spectral Acceleration 5% damping**							
0.010	**-0.52883**	**-0.49429**	**-0.74551**	**-0.49966**	**0.28897**	**-0.10019**	**0.00000**	**6.75**
0.020	-0.52192	-0.48508	-0.73906	-0.48895	0.25144	-0.11006	0.00000	6.75
0.030	-0.45285	-0.41831	-0.66722	-0.42229	0.17976	-0.12858	0.00000	6.75
0.050	**-0.28476**	**-0.25022**	**-0.48462**	**-0.26092**	**0.06369**	**-0.15752**	**0.00000**	**6.75**
0.075	0.00767	0.04912	-0.20578	0.02706	0.01170	-0.17051	0.00000	6.75
0.100	**0.20109**	**0.23102**	**0.03058**	**0.22193**	**0.04697**	**-0.15948**	**0.00000**	**6.75**
0.150	0.46128	0.48661	0.30185	0.49328	0.17990	-0.14539	0.00000	6.75
0.200	**0.57180**	**0.59253**	**0.40860**	**0.61472**	**0.52729**	**-0.12964**	**0.00102**	**6.75**
0.250	0.51884	0.53496	0.33880	0.57747	0.60880	-0.13843	0.08607	6.75
0.300	0.43825	0.44516	0.25356	0.51990	0.64472	-0.15694	0.10601	6.75
0.400	**0.39220**	**0.40602**	**0.21398**	**0.46080**	**0.78610**	**-0.07843**	**0.02262**	**6.75**
0.500	0.18957	0.19878	0.00967	0.26337	0.76837	-0.09054	0.00000	6.75
0.750	-0.21338	-0.19496	-0.49176	-0.10813	0.75179	-0.14053	0.10302	6.75
1.000	**-0.46896**	**-0.43443**	**-0.78465**	**-0.39330**	**0.67880**	**-0.18257**	**0.05393**	**6.75**
1.500	-0.86271	-0.79593	-1.20902	-0.88085	0.70689	-0.25950	0.19082	6.75
2.000	**-1.22652**	**-1.15514**	**-1.57697**	**-1.27669**	**0.77989**	**-0.29657**	**0.29888**	**6.75**
3.000	-1.82979	-1.74690	-2.22584	-1.91814	0.77966	-0.45384	0.67466	6.75
4.000	-2.24656	-2.15906	-2.58228	-2.38168	1.24961	-0.35874	0.79508	6.75
5.000	**-1.28408**	**-1.21270**	**-1.50904**	**-1.41093**	**0.14271**	**-0.39006**	**0.00000**	**8.50**
7.500	-1.43145	-1.31632	-1.81022	-1.59217	0.52407	-0.37578	0.00000	8.50
10.000	**-2.15446**	**-2.16137**	**-2.53323**	**-2.14635**	**0.40387**	**-0.48492**	**0.00000**	**8.50**

7.3 Application of Ground Motion Models in PSHA

The two ground motion prediction equations, **SEA99** and **B&A08**, were used in the site-specific PSHA to predict earthquake ground motion spectra at top of bedrock for occurrence of earthquakes in extensional tectonic regimes. **SEA99** was developed specifically to predict ground motion on normal faults in response to regional extensional stresses. **B&A08** was developed with a flexibility to predict ground motions as a function of style of faulting. This model was operated in the PSHA to make predictions of ground motion amplitudes associated normal slip on faults. **SEA99** described 'bedrock' as shear wave velocity, V_S, greater than 620 m/sec (2,034 ft/sec). **B&A08** incorporates a term that accommodates specification of the local shear wave velocity in the topmost 30 m (98 ft) of geologic material, V_{S30}. **B&A08** was applied in two methods, the first assuming a V_{S30} of 760 m/sec (2,493 ft/sec), and the second assuming a V_{S30} of 1,300 m/sec (4,265 ft/sec).

The EREF site is underlain by basalt bedrock covered with a thin veneer of sediments that ranges in depth from 0 m to 4.3 m (0 ft to 14 ft) at points across the site. Shear wave velocity measurements are not available for the site. Geophysical tests made at the adjacent INL property show that V_{S30} in the top basalt layers ranges from about 1,200 – 1,500 m/sec (4,000 to 5,000 ft/sec) (Payne et al. 2002, Appendix F). This information, included in Appendix B, supports specification of a hard bedrock condition V_{S30} of 1,300 m/sec at the EREF site. Seismic hazard results are provided for **SEA99** and **B&A08** for V_{S30} of 760 m/sec (2,493 ft/sec) and V_{S30} of 1,300 m/sec (4,265 ft/sec).

8.0 Deterministic Response Spectra

Deterministic response spectra are calculated using the **SEA99** and **B&A08** ground motion prediction equations for normal slip on regional faults to compare ground motion predictions of the two attenuation models. The following earthquake scenarios listed in **Table 10** are used. These magnitude-distance scenarios are depicted on **Figure 7** and represent earthquake magnitudes and distances to regional Quaternary Faults listed in **Table 2**.

For each scenario, **SEA99** predictions are mean response spectra for bedrock site conditions. **B&A08** predictions are median response spectra for two bedrock conditions, 1. V_{S30} = 760 m/sec (2,493 ft/sec), and 2. V_{S30} = 1,300 m/sec (4,265 ft/sec). The V_{S30} estimated for the EREF site (Payne et al. 2002) is approximately 1400 m/sec (4,593 ft/sec) based on regional geophysical tests performed on INL property located near the EREF site (Appendix B).

Table 10 – Earthquake Scenarios for Calculation of Deterministic Response Spectra

Deterministic Scenario	Distance, km (mi)	Magnitude M_W
1. Lost River Fault 601 (nearest segment)	98 (61)	7.3
2. Lemhi Fault 602 (nearest segment)	60 (37)	7.0
3. Idaho Rift (3501) nearest segment	10 (6)	6.0

Calculated response spectra for the three scenarios are shown on **Figures 11, 12, and 13**, respectively. **SEA99** and **B&A08** for V_{S30} =760 m/sec (2,493 ft/sec) exhibit similar predictions of bedrock response spectra for the 3 deterministic scenarios. Selecting a higher V_{S30} of 1,300 m/sec (4,265 ft/sec) to characterize bedrock conditions for the **B&A08** ground motion model produces lower amplitude response spectra. Reductions at higher frequencies range from 10% to 20% and from 20% to 50% at lower ground motion frequencies.

9.0 Results of the PSHA

The site specific PSHA was performed using a logic-tree format including 4 seismic source models are three ground motion prediction models. Earthquake activity rates were determined for each source in each of the 4 source zonation models, but were not additionally varied in the hazard assessment. Conservative maximum magnitudes of 7.0 M_W for the ESRP and 7.7 M_W in the surrounding Basin and Range seismic sources were used in the hazard assessment without additional variation.

Following in **Table 11** are weights assigned to the resulting 12 combinations of seismic source models and ground motion prediction models. Each seismic source model was attributed an equal weight. Both the **SEA99** and **B&A08** ground motion models were given an equal weight. The two predictions within **B&A08** for V_{S30} of 760 m/sec (2,493 ft/sec) and 1,300 m/sec (4,265 ft/sec) were equally weighted.

Table 11 – Weights Assigned to Seismic Source and Attenuation Model Combinations

Seismic Source Model	Attenuation Model	Weight
Model 1 – uniform a-value	SEA99	0.125
Model 1 – uniform a-value	B&A08 VS30 = 760 m/sec (2,493 ft/sec)	0.0625
Model 1 – uniform a-value	B&A08 VS30 = 1,300 m/sec (4,265 ft/sec)	0.0625
Model 1 – local a-value	SEA99	0.125
Model 1 – local a-value	B&A08 VS30 = 760 m/sec (2,493 ft/sec)	0.0625
Model 1 – local a-value	B&A08 VS30 = 1,300 m/sec (4,265 ft/sec)	0.0625
Model 2	SEA99	0.125
Model 2	B&A08 VS30 = 760 m/sec (2,493 ft/sec)	0.0625
Model 2	B&A08 VS30 = 1,300 m/sec (4,265 ft/sec)	0.0625
Model 3	SEA99	0.125
Model 3	B&A08 VS30 = 760 m/sec (2,493 ft/sec)	0.0625
Model 3	B&A08 VS30 = 1,300 m/sec (4,265 ft/sec)	0.0625

Results of the PSHA include determinations of probabilities of exceeding peak ground acceleration (PGA) and spectral acceleration (SA) for 5% damping for ground motion periods ranging from .01 to 10.0 seconds. All PSHA results are provided as horizontal accelerations and are for bedrock with near surface shear wave velocity greater than 620 m/sec (2.034 ft/sec) to 760 m/sec (2,493 ft/sec). Results for PGA exceedance probabilities in bedrock for the 12 model combinations are listed in **Table 12**. Results for the **B&A08** ground motion prediction model for bedrock with V_{S30} = 760 m/sec (2,493 ft/sec) are labeled as **Bbc** in **Table 12** implying the same shear wave velocity definition used by NEHRP for the boundary between site conditions B and C, B-C Boundary. Results for V_{S30} = 1,300 m/sec (4,265 ft/sec) are labeled as **Bhr** in **Table 12** implying a hard rock site condition. Regional geophysical data (Payne at al. 2002) support a hard rock condition at the site, but site-specific shear wave velocities currently are not known. As illustrated in Section 8.0, ground motion spectra in bedrock predicted by **B&A08** decrease as V_{S30} increases. Seismic hazard was computed using the B-C boundary site condition, V_{S30} = 760 m/sec (2,493 ft/sec), and the hard rock site condition, V_{S30} = 1,300 m/sec (4,265 ft/sec), to model the uncertainty in site-specific bedrock conditions.

Results of the site-specific PSHA include seismic hazard curves for PGA and spectral accelerations at 5 Hz and 1Hz, and UHRS for annual exceedance frequencies of 2.1×10^{-3} to 10^{-5}. **Tables 12, 13** and **14** list results of the seismic hazard assessment for peak horizontal ground acceleration, spectral acceleration at 5 Hz and spectral acceleration at 1 Hz, respectively. Seismic hazard curves for peak horizontal ground acceleration, spectral acceleration at 5 Hz and spectral acceleration at 1 Hz are plotted on **Figures 14, 15** and **16,** respectively. Shown in **Table 12** and on **Figure 14** is the weighted average result for the 12 analyzed combinations of seismic sources and ground motion models. The weighted result closely matches the individual result for seismic source model 1 (e.g. **Bbc_M1_L**) with the **B&A08** ground motion model for V_{S30} = 760 m/sec (2,493 ft/sec).

The total PGA seismic hazard results and contributions to total hazard from regional seismic source zones and Quaternary Faults are listed in **Table 15** and are illustrated on **Figure 17**. These results are for seismic source model 3 and the **B&A08** ground motion predictions for a V_{S30} = 760 m/sec (2,493 ft/sec) site condition. The predominant source of ground motion hazard is seismic activity located within the ESRP. The predominance of the local seismic source increases as annual exceedance frequency decrease from 10^{-3} to 10^{-5}. As shown on **Figure 17**, impacts from regional Quaternary Faults are minor compared to ground motion impacts attributed to seismic activity within the ESRP. The reason for the negligible ground motion impacts from the Basin and Range faults at the 10^{-3} to 10^{-5} per year probability levels is the high rate of attenuation of ground vibrations generated by slip on normal faults. Spudich et al. (1999, p. 1161) conclude that "extensional regime ground motions are smaller than ground motions in other tectonic regimes." The central location of the EREF site within the ESRP relative to the adjacent Basin and Range faulted areas contributes to the minimized impact of seismic activity in the tectonically active Basin and Range zones.

Total hazard for spectral acceleration at 1 Hz and contributions to this hazard level from regional seismic sources and Quaternary Faults are listed in **Table 16** and plotted on **Figure 18**. Activity within the ESRP and within segments of the Yellowstone Parabola contribute equally to total hazard for lower frequency ground motion for annual exceedance frequency of 10^{-3}. Contribution to total hazard for SA at 1 Hz from the ESRP increases relative to the Yellowstone Parabola for 10^{-4} and 10^{-5} per year probabilities. Contributions to total hazard for SA at 1 Hz from regional Quaternary Faults is shown on **Figure 18** to be minor compared to the ESRP and Yellowstone Parabola seismic zones.

Table 12 – Annual Frequencies of Exceedance for Peak Horizontal Ground Acceleration in Bedrock

Model --->		S99_M1_U	S99_M1_L	S99_M2	S99_M3	Bbc_M1_U	Bbc_M1_L	Bbc_M2	Bbc_M3	Bhr_M1_U	Bhr_M1_L	Bhr_M2	Bhr_M3	Weighted
Weight--->		0.125	0.125	0.125	0.125	0.0625	0.0625	0.0625	0.0625	0.0625	0.0625	0.0625	0.0625	Result
cm/sec^2	in/sec^2	Annual Exceedance Frequency												
9.8	3.9	1.15E-01	7.58E-02	6.43E-02	1.01E-01	4.52E-02	3.00E-02	2.09E-02	4.17E-02	3.43E-02	2.30E-02	1.57E-02	3.16E-02	5.97E-02
49.0	19.3	2.50E-03	2.06E-03	1.62E-03	2.27E-03	2.30E-03	1.75E-03	1.30E-03	2.10E-03	1.44E-03	1.13E-03	8.61E-04	1.32E-03	1.82E-03
73.6	29.0	8.19E-04	7.45E-04	6.59E-04	7.71E-04	8.37E-04	6.74E-04	5.35E-04	7.66E-04	4.98E-04	4.12E-04	3.38E-04	4.57E-04	6.57E-04
98.1	38.6	3.81E-04	3.63E-04	3.41E-04	3.68E-04	3.82E-04	3.20E-04	2.68E-04	3.52E-04	2.18E-04	1.88E-04	1.63E-04	2.03E-04	3.13E-04
122.6	48.3	2.10E-04	2.05E-04	1.98E-04	2.06E-04	2.00E-04	1.73E-04	1.50E-04	1.86E-04	1.11E-04	9.87E-05	8.83E-05	1.04E-04	1.72E-04
147.1	57.9	1.27E-04	1.25E-04	1.23E-04	1.25E-04	1.15E-04	1.02E-04	9.12E-05	1.08E-04	6.22E-05	5.66E-05	5.20E-05	5.90E-05	1.03E-04
196.2	77.2	5.37E-05	5.34E-05	5.29E-05	5.34E-05	4.56E-05	4.20E-05	3.90E-05	4.35E-05	2.37E-05	2.23E-05	2.12E-05	2.29E-05	4.29E-05
245.2	96.5	2.55E-05	2.54E-05	2.53E-05	2.54E-05	2.13E-05	2.02E-05	1.92E-05	2.06E-05	1.07E-05	1.03E-05	9.95E-06	1.05E-05	2.04E-05
294.1	115.8	1.30E-05	1.30E-05	1.30E-05	1.30E-05	1.12E-05	1.07E-05	1.03E-05	1.09E-05	5.41E-06	5.27E-06	5.15E-06	5.33E-06	1.05E-05
392.3	154.4	3.96E-06	3.96E-06	3.95E-06	3.96E-06	3.75E-06	3.66E-06	3.60E-06	3.70E-06	1.71E-06	1.69E-06	1.67E-06	1.70E-06	3.32E-06
490.3	193.0	1.39E-06	1.39E-06	1.39E-06	1.39E-06	1.51E-06	1.49E-06	1.47E-06	1.50E-06	6.51E-07	6.46E-07	6.42E-07	6.48E-07	1.23E-06
980.4	386.0	2.50E-08	2.50E-08	2.50E-08	2.50E-08	5.63E-08	5.62E-08	5.62E-08	5.63E-08	1.94E-08	1.94E-08	1.94E-08	1.94E-08	3.14E-08

Table 13 – Annual Frequencies of Exceedance for Spectral Acceleration at 5 Hz (5% damping) in Bedrock

		Model--->		S99_M1_U	S99_M1_L	S99_M2	S99_M3	Bbc_M1_U	Bbc_M1_L	Bbc_M2	Bbc_M3	Bhr_M1_U	Bhr_M1_L	Bhr_M2	Bhr_M3
		Weight--->		0.125	0.125	0.125	0.125	0.0625	0.0625	0.0625	0.0625	0.0625	0.0625	0.0625	0.0625
SEA99		B&A 2008													
cm/sec^2	in/sec^2	cm/sec^2	in/sec^2	Annual Exceedance Frequency											
15.7	6.2	9.8	3.9	1.85E-01	1.22E-01	1.17E-01	1.56E-01	1.52E-01	9.97E-02	8.44E-02	1.34E-01	1.30E-01	8.55E-02	7.03E-02	1.16E-01
31.4	12.4	49.0	19.3	7.19E-02	4.80E-02	3.97E-02	6.39E-02	1.75E-02	1.20E-02	8.08E-03	1.61E-02	1.27E-02	8.82E-03	5.96E-03	1.17E-02
62.8	24.7	73.6	29.0	1.78E-02	1.24E-02	8.99E-03	1.62E-02	7.81E-03	5.54E-03	3.77E-03	7.19E-03	5.44E-03	3.93E-03	2.71E-03	5.00E-03
157.1	61.8	98.1	38.6	1.63E-03	1.32E-03	1.03E-03	1.50E-03	4.13E-03	3.03E-03	2.12E-03	3.79E-03	2.79E-03	2.09E-03	1.49E-03	2.56E-03
314.2	123.7	122.6	48.3	2.23E-04	2.08E-04	1.90E-04	2.13E-04	2.43E-03	1.83E-03	1.32E-03	2.23E-03	1.60E-03	1.24E-03	9.17E-04	1.47E-03
377.0	148.4	147.1	57.9	1.30E-04	1.24E-04	1.17E-04	1.26E-04	1.54E-03	1.19E-03	8.86E-04	1.41E-03	9.95E-04	7.90E-04	6.05E-04	9.11E-04
471.2	185.5	196.2	77.2	6.63E-05	6.46E-05	6.23E-05	6.50E-05	7.15E-04	5.79E-04	4.54E-04	6.56E-04	4.48E-04	3.72E-04	3.01E-04	4.12E-04
628.6	247.5	245.2	96.5	2.63E-05	2.60E-05	2.56E-05	2.61E-05	3.80E-04	3.19E-04	2.61E-04	3.51E-04	2.33E-04	2.01E-04	1.70E-04	2.16E-04
1570.8	618.4	294.1	115.8	7.00E-07	7.00E-07	6.99E-07	7.00E-07	2.22E-04	1.92E-04	1.63E-04	2.07E-04	1.34E-04	1.19E-04	1.04E-04	1.25E-04
2198.2	865.4	392.3	154.4	1.27E-07	1.27E-07	1.27E-07	1.27E-07	9.14E-05	8.26E-05	7.37E-05	8.63E-05	5.36E-05	4.95E-05	4.53E-05	5.11E-05
3141.0	1236.6	490.3	193.0	1.55E-08	1.55E-08	1.55E-08	1.55E-08	4.46E-05	4.15E-05	3.82E-05	4.26E-05	2.56E-05	2.43E-05	2.28E-05	2.47E-05
6281.3	2473.0	980.4	386.0	1.02E-10	1.02E-10	1.02E-10	1.02E-10	3.94E-06	3.87E-06	3.80E-06	3.89E-06	2.08E-06	2.06E-06	2.03E-06	2.07E-06

Table 14 – Annual Frequencies of Exceedance for Spectral Acceleration at 1 Hz (5% damping) in Bedrock

		Model--->		S99_M1_U	S99_M1_L	S99_M2	S99_M3	Bbc_M1_U	Bbc_M1_L	Bbc_M2	Bbc_M3	Bhr_M1_U	Bhr_M1_L	Bhr_M2	Bhr_M3
		Weight--->		0.125	0.125	0.125	0.125	0.0625	0.0625	0.0625	0.0625	0.0625	0.0625	0.0625	0.0625
SEA99		B&A 2008													
cm/sec^2	in/sec^2	cm/sec^2	in/sec^2	Annual Exceedance Frequency											
3.1	1.2	9.8	3.9	1.57E-01	1.03E-01	9.89E-02	1.33E-01	2.76E-02	1.89E-02	1.60E-02	2.56E-02	1.52E-02	1.05E-02	8.65E-03	1.44E-02
6.3	2.5	49.0	19.3	6.53E-02	4.41E-02	3.77E-02	5.81E-02	1.10E-03	7.75E-04	5.86E-04	1.06E-03	3.83E-04	2.73E-04	2.07E-04	3.64E-04
12.6	4.9	73.6	29.0	2.05E-02	1.45E-02	1.14E-02	1.89E-02	3.50E-04	2.50E-04	1.89E-04	3.32E-04	1.05E-04	7.79E-05	6.08E-05	9.84E-05
31.4	12.4	98.1	38.6	3.10E-03	2.39E-03	1.79E-03	2.92E-03	1.41E-04	1.03E-04	7.98E-05	1.32E-04	3.86E-05	2.98E-05	2.42E-05	3.59E-05
62.8	24.7	122.6	48.3	5.82E-04	4.83E-04	3.70E-04	5.40E-04	6.62E-05	4.99E-05	3.96E-05	6.18E-05	1.70E-05	1.37E-05	1.15E-05	1.59E-05
75.4	29.7	147.1	57.9	3.63E-04	3.07E-04	2.39E-04	3.36E-04	3.47E-05	2.69E-05	2.20E-05	3.23E-05	8.55E-06	7.10E-06	6.19E-06	8.01E-06
94.2	37.1	196.2	77.2	1.99E-04	1.73E-04	1.39E-04	1.84E-04	1.19E-05	9.75E-06	8.38E-06	1.12E-05	2.77E-06	2.44E-06	2.23E-06	2.64E-06
125.7	49.5	245.2	96.5	8.93E-05	8.01E-05	6.69E-05	8.31E-05	5.06E-06	4.32E-06	3.85E-06	4.77E-06	1.13E-06	1.03E-06	9.71E-07	1.09E-06
314.2	123.7	294.1	115.8	5.64E-06	5.48E-06	5.19E-06	5.50E-06	2.47E-06	2.18E-06	2.00E-06	2.35E-06	5.33E-07	4.99E-07	4.79E-07	5.18E-07
439.6	173.1	392.3	154.4	1.85E-06	1.82E-06	1.77E-06	1.83E-06	7.68E-07	7.10E-07	6.76E-07	7.43E-07	1.55E-07	1.49E-07	1.46E-07	1.52E-07
628.2	247.3	490.3	193.0	5.13E-07	5.10E-07	5.04E-07	5.10E-07	3.01E-07	2.86E-07	2.77E-07	2.94E-07	5.66E-08	5.54E-08	5.47E-08	5.61E-08
1256.3	494.6	980.4	386.0	2.76E-08	2.76E-08	2.75E-08	2.76E-08	1.22E-08	1.21E-08	1.21E-08	1.22E-08	1.66E-09	1.65E-09	1.65E-09	1.66E-09

Table 15 – Total PGA Hazard and Contributions from Seismic Sources
Seismic Source Model 3 and Boore and Atkinson GMPE for V_{S30} of 760 m/sec (2,493 ft/sec)

Model		Total		Yparab	Yparab	Yparab	Lost River	Lemhi	Beaverhead	Teton	Grand Valley
cm/sec^2	in/sec^2	Hazard	ESRP	West	North	East	Q-601	Q-602	Q-603	Q-768	Q-726
		Annual Exceedance Frequency									
9.810	3.86	4.17E-02	7.07E-03	1.09E-02	8.11E-03	4.19E-03	2.53E-03	2.51E-03	1.55E-03	1.64E-03	3.75E-03
49.010	19.30	2.10E-03	9.92E-04	5.18E-04	2.08E-04	7.83E-05	8.78E-05	7.15E-05	5.26E-05	1.19E-05	1.10E-04
73.550	28.96	7.66E-04	4.51E-04	1.68E-04	5.58E-05	1.89E-05	2.27E-05	1.74E-05	1.36E-05	1.54E-06	2.59E-05
98.100	38.62	3.52E-04	2.38E-04	6.67E-05	1.91E-05	6.17E-06	7.27E-06	5.30E-06	4.35E-06	2.82E-07	7.69E-06
122.610	48.27	1.86E-04	1.38E-04	3.01E-05	7.61E-06	2.40E-06	2.68E-06	1.88E-06	1.61E-06	6.50E-08	2.66E-06
147.080	57.91	1.08E-04	8.54E-05	1.48E-05	3.36E-06	1.06E-06	1.10E-06	7.44E-07	6.57E-07	1.78E-08	1.03E-06
196.170	77.23	4.35E-05	3.75E-05	4.27E-06	8.10E-07	2.58E-07	2.28E-07	1.46E-07	1.37E-07	1.90E-09	1.95E-07
245.180	96.53	2.06E-05	1.87E-05	1.45E-06	2.39E-07	7.79E-08	5.89E-08	3.61E-08	3.53E-08	2.84E-10	4.65E-08
294.120	115.79	1.09E-05	1.02E-05	5.59E-07	8.13E-08	2.73E-08	1.78E-08	1.05E-08	1.06E-08	5.28E-11	1.31E-08
392.290	154.44	3.70E-06	3.57E-06	1.06E-07	1.26E-08	4.50E-09	2.23E-09	1.24E-09	1.34E-09	1.36E-12	1.48E-09
490.290	193.03	1.50E-06	1.47E-06	2.54E-08	2.59E-09	9.80E-10	3.83E-10	2.03E-10	2.29E-10	0.00E+00	2.31E-10
980.440	386.00	5.63E-08	5.61E-08	1.35E-10	7.70E-12	3.69E-12	2.91E-13	5.68E-14	1.53E-13	0.00E+00	0.00E+00

Table 16 – Total Spectral Acceleration at 1 Hz (5% damping) Hazard and Contributions from Seismic Sources Seismic Source Model 3 and Boore and Atkinson GMPE for V_{S30} of 760 m/sec (2,493 ft/sec)

Model		Total		Yparab	Yparab	Yparab	Lost River	Lemhi	Beaverhead	Teton	Grand Valley
cm/sec^2	in/sec^2	Hazard	ESRP	West	North	East	Q-601	Q-602	Q-603	Q-768	Q-726
9.810	3.86	2.56E-02	3.32E-03	7.36E-03	6.91E-03	1.72E-03	1.23E-03	1.17E-03	7.73E-04	1.33E-03	1.77E-03
49.010	19.30	1.06E-03	2.56E-04	3.17E-04	2.27E-04	3.32E-05	5.56E-05	4.00E-05	3.42E-05	3.01E-05	6.88E-05
73.550	28.96	3.32E-04	1.04E-04	9.79E-05	6.04E-05	8.70E-06	1.58E-05	1.02E-05	9.66E-06	6.33E-06	1.84E-05
98.100	38.62	1.32E-04	5.12E-05	3.75E-05	2.04E-05	2.98E-06	5.53E-06	3.24E-06	3.36E-06	1.74E-06	6.11E-06
122.610	48.27	6.18E-05	2.83E-05	1.65E-05	8.11E-06	1.21E-06	2.21E-06	1.21E-06	1.34E-06	5.69E-07	2.35E-06
147.080	57.91	3.23E-05	1.69E-05	7.99E-06	3.59E-06	5.48E-07	9.81E-07	5.04E-07	5.92E-07	2.12E-07	1.00E-06
196.170	77.23	1.12E-05	7.10E-06	2.28E-06	8.88E-07	1.42E-07	2.38E-07	1.11E-07	1.43E-07	3.87E-08	2.29E-07
245.180	96.53	4.77E-06	3.45E-06	7.86E-07	2.73E-07	4.52E-08	7.08E-08	3.06E-08	4.26E-08	9.19E-09	6.52E-08
294.120	115.79	2.35E-06	1.85E-06	3.09E-07	9.77E-08	1.68E-08	2.45E-08	9.94E-09	1.47E-08	2.62E-09	2.17E-08
392.290	154.44	7.43E-07	6.49E-07	6.23E-08	1.70E-08	3.09E-09	3.98E-09	1.46E-09	2.38E-09	3.08E-10	3.30E-09
490.290	193.03	2.94E-07	2.71E-07	1.62E-08	3.93E-09	7.51E-10	8.62E-10	2.91E-10	5.17E-10	5.05E-11	6.78E-10
980.440	386.00	1.22E-08	1.20E-08	1.29E-10	1.98E-11	4.55E-12	2.73E-12	2.91E-13	1.63E-12	0.00E+00	1.19E-12

9.1 Uniform Hazard Response Spectra

Horizontal Component UHRS

Uniform hazard response spectra determined for the EREF site are described in this section. **Tables 18, 19, 20** and **21** provide lists of horizontal motion UHRS ordinates in bedrock for annual exceedance frequencies of 2.1×10^{-3}, 10^{-3}, 10^{-4} and 10^{-5}, respectively. These annual probability levels correspond to mean ground motion return periods of 475, 1,000, 10,000, and 100,000 years, respectively. Results for the 12 combinations of seismic source models and ground motion models are listed in the tables. Results for the **SEA99** ground motion model include PGA and SA (5% damping) for the period range of 0.05 second (20 Hz) to 2.0 seconds (0.5 Hz). Similarly, the **B&A08** ground motion model provides results for PGA and SA (5% damping) over a broader period band from 0.01 second (100 Hz) to 10 seconds (0.1 Hz). A weighted average is listed in the tables for PGA and for 6 common periods for the 2 ground motion models in the band from 0.05 second to 2.0 seconds. **Figures 19, 20, 21**, and **22** illustrate horizontal component UHRS in bedrock for the EREF site for annual exceedance frequencies of 2.1×10^{-3}, 10^{-3}, 10^{-4}, and 10^{-5}, respectively. The weighted results are shown on the figures as dashed curves. The weighted results closely match the individual uniform hazard spectrum determined for seismic source model 1 and the **B&A08** ground motion model for V_{S30} = 760 m/sec (2,493 ft/sec).

Peak horizontal ground acceleration and spectral acceleration amplitudes for the 2.1×10^{-3} to 10^{-5} per year UHRS in bedrock are summarized below in **Table 17**. Peak values shown below are weighted results for the 12 combinations of seismic source zones and ground motion models.

Table 17 – Uniform Hazard Response Spectra – Peak Horizontal Amplitudes in Bedrock

Annual Probability of Exceedance	Peak Horizontal Ground Acceleration	Spectral Acceleration (5% damping ratio)	Pseudo-Relative Velocity (5% damping)
2.1×10^{-3}	44.69 cm/sec^2 0.046 g	119.92 cm/sec^2 (5 Hz) 0.122 g	5.21 cm/sec (2.5 Hz) 2.05 in/sec (2.5 Hz)
10^{-3}	61.37 cm/sec^2 0.063 g	161.15 cm/sec^2 (5 Hz) 0.164 g	6.96 cm/sec (2.5 Hz) 2.74 in/sec (2.5 Hz)
10^{-4}	147.09 cm/sec^2 0.150 g	373.09 cm/sec^2 (5 Hz) 0.381 g	15.97 cm/sec (2.5 Hz) 6.29 in/sec (2.5 Hz)
10^{-5}	293.61 cm/sec^2 0.299 g	743.50 cm/sec^2 (5 Hz) 0.758 g	33.53 cm/sec (1.0 Hz) 13.20 in/sec (1.0 Hz)

Vertical Component UHRS

Ground motion equations used in the probabilistic seismic hazard assessment predict horizontal component peak accelerations and spectra accelerations in bedrock for 5% damping. Vertical component response spectra for 5 % damping in bedrock are determined using the guidance provided in Bozorgnia and Campbell (2004). Bozorgnia and Campbell (2004) determined that the ratio of vertical to horizontal component response spectra is a "strong function of natural period, source-to-site distance and local geology." The following figure (Ibid., Fig. 7, p. 194) illustrates a current trend for definition of the V/H ratio. Shown are V/H ratios for firm rock, hard rock, and very firm soil for source to site distances of 60 km (37.3 mi) and ≤ 20 km (≤ 12.4 mi). V/H ratio increases as earthquake source to site decreases.

Regional tectonics and seismicity for the EREF site area support a low level of local seismic activity and a greater likelihood that seismic ground motion would result from earthquakes located in the surrounding Basin and Range tectonic provinces located greater than 60 km (37.3 mi) from the EREF site. The V/H ratio shown below for a source distance of 60 km (37.3 mi) for short period (0.04 sec to 0.1 sec) motion is 0.67 and is 0.5 for longer period (.3 sec to 3.0 sec) motion. The V/H ratio follows a log-linear ramp between periods of 0.1 sec to 0.3 sec.

The recommended V/H ratio for development of vertical component response spectra for the EREF site is 0.666 (i.e. 2/3) for all periods. Results shown below (Ibid.) support a smaller ratio of 0.5 for longer period motion; however, the limit of 2/3 for the V/H ratio is selected for all periods to be aligned with smallest ratio established in historical regulatory positions (e.g. USAEC, 1973, Regulatory Guide 1.60).

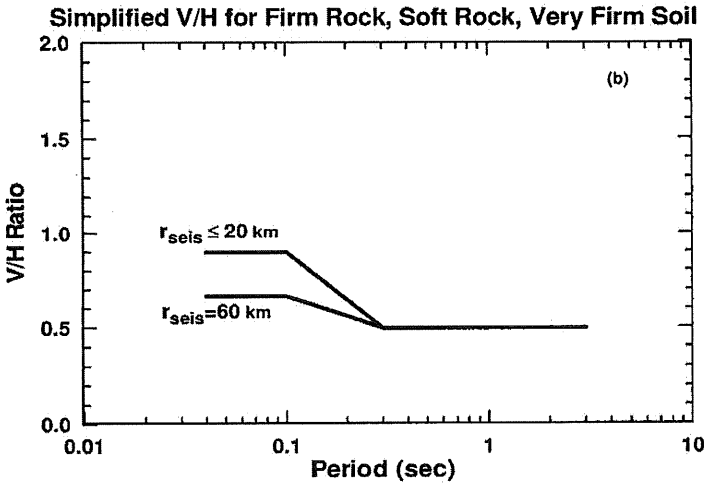

Fig. 7. Simplified V/H response spectral ratio developed in this study.

Recommended Horizontal and Vertical Design Response Spectra

Recommended horizontal component and vertical component design response spectra for a critical damping ratio of 5% in bedrock for annual probabilities of exceedance of 2.1×10^{-3}, 10^{-3}, 10^{-4}, and 10^{-5} are listed on **Tables 22** and **23**, respectively. The upper half of each table lists the response spectra as peak ground acceleration (cm/sec^2) and as pseudo-relative velocity (cm/sec) for 5% damping. The lower half of each table shows amplitudes as spectral accelerations (cm/sec^2) for 5% damping. Also include in the tables are results for case **Bbc_M1_L** that produced UHRS that are close to the weighted result of all 12 cases examined in the psha.

Vertical component response spectra (**Table 23**) were determined using a V/H ratio of 2/3 applied to horizontal component response spectra listed in **Table 22**.

Table 18 – Uniform Hazard Response Spectra for Annual Exceedance Frequency of 2.1×10^{-3}

		Weights-->	0.125	0.125	0.125	0.125	0.0625	0.0625	0.0625	0.0625	0.0625	0.0625	0.0625	0.0625	Weighted
		Model-->	S99_M1_U	S99_M1_L	S99_M2	S99_M3	Bbc_M1_U	Bbc_M1_L	Bbc_M2	Bbc_M3	Bhr_M1_U	Bhr_M1_L	Bhr_M2	Bhr_M3	Result
Period	Frequency	Param	SEA 99				Boore & Atkinson (2008) Vs30=760 m/s				Boore & Atkinson (2008) Vs30=1300 m/s				
(sec)	(Hz)	*(cm/sec^2)	Model1	Model 1	Model 2	Model 3	Model 1	Model 1	Model 2	Model 3	Model 1	Model 1	Model 2	Model 3	
		**(cm/sec)	uniform a	local a			uniform a	local a			uniform a	local a			
0.01	100.00	pga*	52.22	48.61	43.74	50.47	50.77	44.18	37.00	48.96	40.41	35.10	29.85	38.63	44.69
0.01	100.00	psrv 5%**	0.083	0.077	0.070	0.080	0.081	0.071	0.059	0.078	0.065	0.056	0.048	0.062	
0.05	20.00	psrv 5%**	0.416	0.387	0.348	0.402	0.528	0.469	0.403	0.506	0.451	0.403	0.339	0.433	0.415
0.10	10.00	psrv 5%**	1.850	1.670	1.460	1.780	1.680	1.504	1.289	1.606	1.468	1.314	1.128	1.402	1.557
0.20	5.00	psrv 5%**	4.530	4.130	3.700	4.390	4.136	3.673	3.133	3.994	3.499	3.114	2.648	3.379	3.817
0.40	2.50	psrv 5%**	6.120	5.580	4.950	5.960	6.002	5.258	4.524	5.874	4.591	4.009	3.452	4.490	5.214
1.00	1.00	psrv 5%**	5.870	5.290	4.620	5.720	5.645	4.716	4.187	5.516	3.700	3.170	2.870	3.614	4.776
2.00	0.50	psrv 5%**	5.990	5.330	4.680	5.840	5.176	4.437	4.151	5.071	3.708	3.244	3.008	3.657	4.758
5.00	0.20	psrv 5%**					5.101	4.210	4.019	4.997	3.430	2.737	2.594	3.350	
10.00	0.10	psrv 5%**					3.804	3.167	3.088	3.724	2.722	2.180	2.133	2.658	

		Weights-->	0.125	0.125	0.125	0.125	0.0625	0.0625	0.0625	0.0625	0.0625	0.0625	0.0625	0.0625	Weighted
		Model-->	S99_M1_U	S99_M1_L	S99_M2	S99_M3	Bbc_M1_U	Bbc_M1_L	Bbc_M2	Bbc_M3	Bhr_M1_U	Bhr_M1_L	Bhr_M2	Bhr_M3	Result
Period	Frequency	Param	SEA 99				Boore & Atkinson (2008) Vs30=760 m/s				Boore & Atkinson (2008) Vs30=1300 m/s				
(sec)	(Hz)	(cm/sec^2)	Model1	Model 1	Model 2	Model 3	Model 1	Model 1	Model 2	Model 3	Model 1	Model 1	Model 2	Model 3	
			uniform a	local a			uniform a	local a			uniform a	local a			
0.01	100.00	pga	52.22	48.61	43.74	50.47	50.77	44.18	37.00	48.96	40.41	35.10	29.85	38.63	44.69
0.01	100.00	sa 5%					51.12	44.56	37.30	49.31	40.77	35.39	30.08	38.96	
0.05	20.00	sa 5%	52.22	48.61	43.74	50.47	66.32	58.97	50.63	63.55	56.72	50.65	42.57	54.43	52.12
0.10	10.00	sa 5%	116.24	104.93	91.73	111.84	105.54	94.53	80.99	100.89	92.25	82.56	70.86	88.09	97.82
0.20	5.00	sa 5%	142.31	129.75	116.24	137.92	129.93	115.40	98.43	125.48	109.93	97.82	83.18	106.14	119.92
0.40	2.50	sa 5%	96.13	87.65	77.75	93.62	94.28	82.59	71.06	92.27	72.11	62.98	54.23	70.53	81.90
1.00	1.00	sa 5%	36.88	33.24	29.03	35.94	35.47	29.63	26.31	34.66	23.25	19.92	18.03	22.71	30.01
2.00	0.50	sa 5%	18.82	16.74	14.70	18.35	16.26	13.94	13.04	15.93	11.65	10.19	9.45	11.49	14.95
5.00	0.20	sa 5%					6.41	5.29	5.05	6.28	4.31	3.44	3.26	4.21	
10.00	0.10	sa 5%					2.39	1.99	1.94	2.34	1.71	1.37	1.34	1.67	

SI to customary unit conversions: 1 in/sec = 2.54 cm/sec; 1 cm/sec = 0.3937 in/sec

Table 19 – Uniform Hazard Response Spectra for Annual Exceedance Frequency of 10^{-3}

		Weights-->	0.125	0.125	0.125	0.125	0.0625	0.0625	0.0625	0.0625	0.0625	0.0625	0.0625	0.0625	Weighted
		Model-->	S99_M1_U	S99_M1_L	S99_M2	S99_M3	Bbc_M1_U	Bbc_M1_L	Bbc_M2	Bbc_M3	Bhr_M1_U	Bhr_M1_L	Bhr_M2	Bhr_M3	Result
Period	Frequency	Param	SEA 99				Boore & Atkinson (2008) Vs30=760 m/s				Boore & Atkinson (2008) Vs30=1300 m/s				
(sec)	(Hz)	*(cm/sec^2)	Model1	Model 1	Model 2	Model 3	Model 1	Model 1	Model 2	Model 3	Model 1	Model 1	Model 2	Model 3	
		**(cm/sec)	uniform a	local a			uniform a	local a			uniform a	local a			
0.01	100.00	pga*	68.39	65.41	60.96	66.69	68.45	62.18	55.17	66.04	56.32	51.41	45.08	54.44	61.37
0.01	100.00	psrv 5%**	0.109	0.104	0.097	0.106	0.110	0.100	0.088	0.106	0.090	0.082	0.072	0.087	
0.05	20.00	psrv 5%**	0.544	0.521	0.485	0.531	0.718	0.657	0.588	0.692	0.615	0.563	0.501	0.593	0.568
0.10	10.00	psrv 5%**	2.510	2.330	2.110	2.440	2.283	2.105	1.892	2.196	1.996	1.841	1.654	1.921	2.167
0.20	5.00	psrv 5%**	5.920	5.550	5.060	5.770	5.504	5.020	4.430	5.326	4.671	4.254	3.751	4.517	5.130
0.40	2.50	psrv 5%**	8.020	7.450	6.730	7.820	7.960	7.123	6.231	7.794	6.084	5.440	4.762	5.950	6.961
1.00	1.00	psrv 5%**	7.990	7.290	6.460	7.760	8.074	6.856	6.011	7.963	5.122	4.399	3.952	5.005	6.649
2.00	0.50	psrv 5%**	8.190	7.380	6.520	7.970	7.028	6.013	5.596	6.872	4.845	4.234	3.969	4.762	6.465
5.00	0.20	psrv 5%**					7.361	6.000	5.690	7.186	4.854	4.074	3.883	4.759	
10.00	0.10	psrv 5%**					5.411	4.456	4.329	5.284	3.852	3.247	3.167	3.772	

		Weights	0.125	0.125	0.125	0.125	0.0625	0.0625	0.0625	0.0625	0.0625	0.0625	0.0625	0.0625	Weighted
		Model	S99_M1_U	S99_M1_L	S99_M2	S99_M3	Bbc_M1_U	Bbc_M1_L	Bbc_M2	Bbc_M3	Bhr_M1_U	Bhr_M1_L	Bhr_M2	Bhr_M3	Result
Period	Frequency	Param	SEA 99				Boore & Atkinson (2008) Vs30=760 m/s				Boore & Atkinson (2008) Vs30=1300 m/s				
(sec)	(Hz)	(cm/sec^2)	Model1	Model 1	Model 2	Model 3	Model 1	Model 1	Model 2	Model 3	Model 1	Model 1	Model 2	Model 3	
			uniform a	local a			uniform a	local a			uniform a	local a			
0.01	100.00	pga	68.39	65.41	60.96	66.69	68.45	62.18	55.17	66.04	56.32	51.41	45.08	54.44	61.37
0.01	100.00	sa 5%					69.00	62.66	55.57	66.57	56.75	51.79	45.48	54.85	
0.05	20.00	sa 5%	68.39	65.41	60.96	66.69	90.19	82.58	73.94	86.91	77.24	70.73	62.99	74.51	71.37
0.10	10.00	sa 5%	157.71	146.40	132.58	153.31	143.42	132.29	118.89	137.99	125.42	115.66	103.91	120.70	136.14
0.20	5.00	sa 5%	185.98	174.36	158.96	181.27	172.90	157.72	139.18	167.33	146.75	133.65	117.84	141.92	161.15
0.40	2.50	sa 5%	125.98	117.02	105.71	122.84	125.04	111.88	97.87	122.43	95.56	85.45	74.80	93.46	109.35
1.00	1.00	sa 5%	50.20	45.80	40.59	48.76	50.73	43.08	37.77	50.03	32.18	27.64	24.83	31.45	41.78
2.00	0.50	sa 5%	25.73	23.18	20.48	25.04	22.08	18.89	17.58	21.59	15.22	13.30	12.47	14.96	20.31
5.00	0.20	sa 5%					9.25	7.54	7.15	9.03	6.10	5.12	4.88	5.98	
10.00	0.10	sa 5%					3.40	2.80	2.72	3.32	2.42	2.04	1.99	2.37	

SI to customary unit conversions: 1 in/sec = 2.54 cm/sec; 1 cm/sec = 0.3937 in/sec

Table 20 - Uniform Hazard Response Spectra for Annual Exceedance Frequency of 10^{-4}

		Weights-->	0.125	0.125	0.125	0.125	0.0625	0.0625	0.0625	0.0625	0.0625	0.0625	0.0625	0.0625	Weighted
		Model-->	S99_M1_U	S99_M1_L	S99_M2	S99_M3	Bbc_M1_U	Bbc_M1_L	Bbc_M2	Bbc_M3	Bhr_M1_U	Bhr_M1_L	Bhr_M2	Bhr_M3	Result
Period	Frequency	Param	SEA 99				Boore & Atkinson (2008) Vs30=760 m/s				Boore & Atkinson (2008) Vs30=1300 m/s				
(sec)	(Hz)	*(cm/sec^2)	Model1	Model 1	Model 2	Model 3	Model 1	Model 1	Model 2	Model 3	Model 1	Model 1	Model 2	Model 3	
		**(cm/sec)	uniform a	local a			uniform a	local a			uniform a	local a			
0.01	100.00	pga*	159.28	158.70	157.69	158.78	153.57	148.04	142.20	150.61	126.66	122.04	117.16	124.20	147.09
0.01	100.00	psrv 5%**					0.247	0.238	0.228	0.242	0.203	0.196	0.188	0.199	
0.05	20.00	psrv 5%**	1.268	1.263	1.255	1.264	1.664	1.615	1.568	1.636	1.423	1.380	1.338	1.399	1.383
0.10	10.00	psrv 5%**	6.250	6.150	6.020	6.180	5.366	5.246	5.119	5.292	4.700	4.595	4.484	4.635	5.540
0.20	5.00	psrv 5%**	13.100	12.930	12.690	12.980	12.130	11.699	11.176	11.893	10.261	9.907	9.482	10.067	11.876
0.40	2.50	psrv 5%**	17.860	17.470	16.860	17.610	17.042	16.115	15.009	16.699	13.031	12.323	11.465	12.771	15.878
1.00	1.00	psrv 5%**	19.210	18.410	17.070	18.710	17.275	15.766	14.482	16.942	11.876	10.797	9.923	11.649	15.969
2.00	0.50	psrv 5%**	19.650	18.560	16.930	19.130	17.402	15.428	14.120	17.039	11.093	9.693	9.037	10.810	15.823
5.00	0.20	psrv 5%**					15.868	13.560	12.971	15.414	10.958	9.533	9.151	10.695	
10.00	0.10	psrv 5%**					13.496	11.332	10.918	13.114	9.486	8.117	7.846	9.247	

		Weights	0.125	0.125	0.125	0.125	0.0625	0.0625	0.0625	0.0625	0.0625	0.0625	0.0625	0.0625	Weighted
		Model	S99_M1_U	S99_M1_L	S99_M2	S99_M3	Bbc_M1_U	Bbc_M1_L	Bbc_M2	Bbc_M3	Bhr_M1_U	Bhr_M1_L	Bhr_M2	Bhr_M3	Result
Period	Frequency	Param	SEA 99				Boore & Atkinson (2008) Vs30=760 m/s				Boore & Atkinson (2008) Vs30=1300 m/s				
(sec)	(Hz)	(cm/sec^2)	Model1	Model 1	Model 2	Model 3	Model 1	Model 1	Model 2	Model 3	Model 1	Model 1	Model 2	Model 3	
			uniform a	local a			uniform a	local a			uniform a	local a			
0.01	100.00	pga	159.28	158.70	157.69	158.78	153.57	148.04	142.20	150.61	126.66	122.04	117.16	124.20	147.09
0.01	100.00	sa 5%					154.97	149.36	143.52	151.98	127.83	123.17	118.25	125.34	
0.05	20.00	sa 5%	159.28	158.70	157.69	158.78	209.05	202.97	197.04	205.63	178.79	173.45	168.19	175.80	173.74
0.10	10.00	sa 5%	392.70	386.42	378.25	388.30	337.17	329.60	321.63	332.49	295.31	288.74	281.71	291.24	348.08
0.20	5.00	sa 5%	411.55	406.21	398.67	407.78	381.06	367.54	351.11	373.64	322.36	311.23	297.89	316.25	373.09
0.40	2.50	sa 5%	280.54	274.42	264.84	276.62	267.69	253.14	235.76	262.30	204.69	193.57	180.09	200.60	249.42
1.00	1.00	sa 5%	120.70	115.67	107.25	117.56	108.54	99.06	90.99	106.45	74.62	67.84	62.35	73.19	100.34
2.00	0.50	sa 5%	61.73	58.31	53.19	60.10	54.67	48.47	44.36	53.53	34.85	30.45	28.39	33.96	49.71
5.00	0.20	sa 5%					19.94	17.04	16.30	19.37	13.77	11.98	11.50	13.44	
10.00	0.10	sa 5%					8.48	7.12	6.86	8.24	5.96	5.10	4.93	5.81	

SI to customary unit conversions: 1 in/sec = 2.54 cm/sec; 1 cm/sec = 0.3937 in/sec

Table 21 - Uniform Hazard Response Spectra for Annual Exceedance Frequency of 10^{-5}

		Weights-->	0.125	0.125	0.125	0.125	0.0625	0.0625	0.0625	0.0625	0.0625	0.0625	0.0625	0.0625	Weighted
		Model-->	S99_M1_U	S99_M1_L	S99_M2	S99_M3	Bbc_M1_U	Bbc_M1_L	Bbc_M2	Bbc_M3	Bhr_M1_U	Bhr_M1_L	Bhr_M2	Bhr_M3	Result
Period	Frequency	Param	SEA 99				Boore & Atkinson (2008) Vs30=760 m/s				Boore & Atkinson (2008) Vs30=1300 m/s				
(sec)	(Hz)	*(cm/sec^2)	Model1	Model 1	Model 2	Model 3	Model 1	Model 1	Model 2	Model 3	Model 1	Model 1	Model 2	Model 3	
		**(cm/sec)	uniform a	local a			uniform a	local a			uniform a	local a			
0.01	100.00	pga*	313.57	313.52	313.38	313.52	302.73	299.55	296.87	300.90	249.68	247.05	244.79	248.17	293.61
0.01	100.00	psrv 5%**					0.487	0.482	0.477	0.484	0.402	0.397	0.394	0.399	
0.05	20.00	psrv 5%**	2.495	2.495	2.494	2.495	3.424	3.401	3.382	3.411	2.930	2.909	2.892	2.918	2.827
0.10	10.00	psrv 5%**	13.860	13.840	13.810	13.840	11.099	11.041	10.984	11.062	9.717	9.670	9.626	9.687	12.099
0.20	5.00	psrv 5%**	25.540	25.490	25.410	25.500	23.914	23.653	23.344	23.748	20.231	20.021	19.775	20.094	23.666
0.40	2.50	psrv 5%**	35.990	35.770	35.410	35.830	33.095	32.456	31.755	32.759	25.370	24.875	24.297	25.110	32.232
1.00	1.00	psrv 5%**	41.340	40.710	39.520	40.860	32.697	31.002	29.614	32.140	22.458	21.282	20.348	22.070	33.529
2.00	0.50	psrv 5%**	41.770	40.680	38.790	41.070	33.273	30.383	28.858	32.515	22.473	20.480	19.468	21.941	33.376
5.00	0.20	psrv 5%**					33.542	28.067	26.658	32.125	21.191	18.207	17.435	20.459	
10.00	0.10	psrv 5%**					25.115	21.772	21.088	24.398	18.494	16.218	15.725	18.000	

		Weights	0.125	0.125	0.125	0.125	0.0625	0.0625	0.0625	0.0625	0.0625	0.0625	0.0625	0.0625	Weighted
		Model	S99_M1_U	S99_M1_L	S99_M2	S99_M3	Bbc_M1_U	Bbc_M1_L	Bbc_M2	Bbc_M3	Bhr_M1_U	Bhr_M1_L	Bhr_M2	Bhr_M3	Result
Period	Frequency	Param	SEA 99				Boore & Atkinson (2008) Vs30=760 m/s				Boore & Atkinson (2008) Vs30=1300 m/s				
(sec)	(Hz)	(cm/sec^2)	Model1	Model 1	Model 2	Model 3	Model 1	Model 1	Model 2	Model 3	Model 1	Model 1	Model 2	Model 3	
			uniform a	local a			uniform a	local a			uniform a	local a			
0.01	100.00	pga	313.57	313.52	313.38	313.52	302.73	299.55	296.87	300.90	249.68	247.05	244.79	248.17	293.61
0.01	100.00	sa 5%					305.91	302.66	299.91	304.04	252.34	249.65	247.36	250.79	
0.05	20.00	sa 5%	313.57	313.52	313.38	313.52	430.29	427.36	424.99	428.60	368.20	365.60	363.48	366.70	355.20
0.10	10.00	sa 5%	870.85	869.59	867.71	869.59	697.40	693.71	690.15	695.04	610.52	607.60	604.83	608.65	760.21
0.20	5.00	sa 5%	802.36	800.79	798.28	801.11	751.29	743.08	733.36	746.08	635.57	628.97	621.24	631.28	743.50
0.40	2.50	sa 5%	565.33	561.87	556.22	562.82	519.86	509.81	498.81	514.58	398.51	390.74	381.65	394.42	506.30
1.00	1.00	sa 5%	259.75	255.79	248.31	256.73	205.44	194.79	186.07	201.94	141.11	133.72	127.85	138.67	210.67
2.00	0.50	sa 5%	131.22	127.80	121.86	129.03	104.53	95.45	90.66	102.15	70.60	64.34	61.16	68.93	104.85
5.00	0.20	sa 5%					42.15	35.27	33.50	40.37	26.63	22.88	21.91	25.71	
10.00	0.10	sa 5%					15.78	13.68	13.25	15.33	11.62	10.19	9.88	11.31	

SI to customary unit conversions: 1 in/sec = 2.54 cm/sec; 1 cm/sec = 0.3937 in/sec

Table 22 – Horizontal Component Uniform Hazard Response Spectra for Annual Exceedance Frequencies of 2.1 x 10^{-3} to 1.0 x 10^{-5}

Period	Frequency	Param	p_E= 0.0021/yr (475 yr)		p_E= 0.001/yr (1,000 yr)		p_E= 0.0001/yr (10,000 yr)		p_E= 0.00001/yr (100,000 yr)	
(sec)	(Hz)	*(cm/sec^2) **(cm/sec)	Weighted Result	Model Bbc_M1_L	Weighted Result	Model Bbc_M1_L	Weighted Result	Model Bbc_M1_L	Weighted Result	Model Bbc_M1_L
0.01	100.00	pga*	44.69	44.18	61.37	62.18	147.09	148.04	293.61	299.55
0.01	100.00	psrv 5%**	0.07	0.07	0.10	0.10	0.23	0.24	0.47	0.48
0.05	20.00	psrv 5%**	0.41	0.47	0.57	0.66	1.38	1.62	2.83	3.40
0.10	10.00	psrv 5%**	1.56	1.50	2.17	2.11	5.54	5.25	12.10	11.04
0.20	5.00	psrv 5%**	3.82	3.67	5.13	5.02	11.88	11.70	23.67	23.65
0.40	2.50	psrv 5%**	5.21	5.26	6.96	7.12	15.88	16.12	32.23	32.46
1.00	1.00	psrv 5%**	4.78	4.72	6.65	6.86	15.97	15.77	33.53	31.00
2.00	0.50	psrv 5%**	4.76	4.44	6.46	6.01	15.82	15.43	33.38	30.38
5.00	0.20	psrv 5%**		4.21		6.00		13.56		28.07
10.00	0.10	psrv 5%**		3.17		4.46		11.33		21.77

Period	Frequency	Param	p_E= 0.0021/yr (475 yr)		p_E= 0.001/yr (1,000 yr)		p_E= 0.0001/yr (10,000 yr)		p_E= 0.00001/yr (100,000 yr)	
(sec)	(Hz)	(cm/sec^2)	Weighted Result	Model Bbc_M1_L	Weighted Result	Model Bbc_M1_L	Weighted Result	Model Bbc_M1_L	Weighted Result	Model Bbc_M1_L
0.01	100.00	pga	44.69	44.18	61.37	62.18	147.09	148.04	293.61	299.55
0.01	100.00	sa 5%		44.56		62.66		149.36		302.66
0.05	20.00	sa 5%	52.12	58.97	71.37	82.58	173.74	202.97	355.20	427.36
0.10	10.00	sa 5%	97.82	94.53	136.14	132.29	348.08	329.60	760.21	693.71
0.20	5.00	sa 5%	119.92	115.40	161.15	157.72	373.09	367.54	743.50	743.08
0.40	2.50	sa 5%	81.90	82.59	109.35	111.88	249.42	253.14	506.30	509.81
1.00	1.00	sa 5%	30.01	29.63	41.78	43.08	100.34	99.06	210.67	194.79
2.00	0.50	sa 5%	14.95	13.94	20.31	18.89	49.71	48.47	104.85	95.45
5.00	0.20	sa 5%		5.29		7.54		17.04		35.27
10.00	0.10	sa 5%		1.99		2.80		7.12		13.68

Table 23 – Vertical Component Uniform Hazard Response Spectra for Annual Exceedance Frequencies of 2.1 x 10^{-3} to 1.0 x 10^{-5}

Period	Frequency	Param	p_E= 0.0021/yr (475 yr)		p_E= 0.001/yr (1,000 yr)		p_E= 0.0001/yr (10,000 yr)		p_E= 0.00001/yr (100,000 yr)	
(sec)	(Hz)	*(cm/sec^2) **(cm/sec)	Weighted Result	Model Bbc_M1_L	Weighted Result	Model Bbc_M1_L	Weighted Result	Model Bbc_M1_L	Weighted Result	Model Bbc_M1_L
0.01	100.00	pga*	29.79	29.45	40.92	41.45	98.06	98.69	195.74	199.70
0.01	100.00	psrv 5%**	0.05	0.05	0.07	0.07	0.16	0.16	0.31	0.32
0.05	20.00	psrv 5%**	0.28	0.31	0.38	0.44	0.92	1.08	1.88	2.27
0.10	10.00	psrv 5%**	1.04	1.00	1.44	1.40	3.69	3.50	8.07	7.36
0.20	5.00	psrv 5%**	2.54	2.45	3.42	3.35	7.92	7.80	15.78	15.77
0.40	2.50	psrv 5%**	3.48	3.51	4.64	4.75	10.59	10.74	21.49	21.64
1.00	1.00	psrv 5%**	3.18	3.14	4.43	4.57	10.65	10.51	22.35	20.67
2.00	0.50	psrv 5%**	3.17	2.96	4.31	4.01	10.55	10.29	22.25	20.26
5.00	0.20	psrv 5%**		2.81		4.00		9.04		18.71
10.00	0.10	psrv 5%**		2.11		2.97		7.55		14.51

Period	Frequency	Param	p_E= 0.0021/yr (475 yr)		p_E= 0.001/yr (1,000 yr)		p_E= 0.0001/yr (10,000 yr)		p_E= 0.00001/yr (100,000 yr)	
(sec)	(Hz)	(cm/sec^2)	Weighted Result	Model Bbc_M1_L	Weighted Result	Model Bbc_M1_L	Weighted Result	Model Bbc_M1_L	Weighted Result	Model Bbc_M1_L
0.01	100.00	pga	29.79	29.45	40.92	41.45	98.06	98.69	195.74	199.70
0.01	100.00	sa 5%		29.71		41.77		99.57		201.77
0.05	20.00	sa 5%	34.75	39.31	47.58	55.05	115.83	135.31	236.80	284.91
0.10	10.00	sa 5%	65.22	63.02	90.76	88.19	232.05	219.73	506.81	462.47
0.20	5.00	sa 5%	79.95	76.93	107.43	105.15	248.73	245.03	495.66	495.39
0.40	2.50	sa 5%	54.60	55.06	72.90	74.59	166.28	168.76	337.54	339.87
1.00	1.00	sa 5%	20.01	19.75	27.85	28.72	66.89	66.04	140.45	129.86
2.00	0.50	sa 5%	9.97	9.29	13.54	12.59	33.14	32.31	69.90	63.63
5.00	0.20	sa 5%		3.53		5.03		11.36		23.51
10.00	0.10	sa 5%		1.33		1.87		4.75		9.12

10.0 Comparison of PSHA Results with USGS (2008) and INL Seismic Hazard Estimates

Results of the site-specific PSHA are compared to the USGS (2008) National Seismic Hazard Maps (Petersen et al, 2008). The USGS 2008 update provides seismic hazard values for PGA and SA at 5 Hz, 3 Hz and 1 Hz (5% damping) for a national grid of sites. The USGS grid site nearest to the EREF site is at coordinates -112.45^{O} W. Longitude and 43.6^{O} N. Latitude. **Table 24** lists USGS 2008 seismic hazard results for earthquake ground motion return periods from 475 years to 100,000 years. **Figure 25** shows the USGS 2008 PGA seismic hazard map for 5% probability of exceedance in 50 years (10^{-3} per year probability). The EREF site is situated just inside the 0.08 g PGA contour line. **Figure 26** provides a comparison of site-specific and USGS 2008 seismic hazard curves for PGA and for SA at 5 Hz and 1 Hz.

Table 24 – USGS (2008) Seismic Hazard Results for Vicinity of EREF Site

USGS (2008) Seismic Hazard for -112.45 W, 43.6N						
Period, sec	Frequency, Hz	475 yr p=10% in 50 yr	1,000 yr p=5% in 50 yr	2,500 yr p=2% in 50 yr	10,000 yr p=0.5% in 50 yr	100,000 yr p=.05%in 50 yr
		pga, sa, g	pga sa, g	pga, sa, g	pga, sa, g	pga, sa, g
	PGA	0.0600	0.0790	0.1090	0.1800	0.4220
	SA (5%)					
0.0303	33.00	0.0600	0.0790	0.1090	0.1800	0.4220
0.20	5.00	0.1540	0.2020	0.2780	0.4550	1.0470
0.33	3.00	0.1360	0.1760	0.2380	0.3750	0.8320
1.00	1.00	0.0527	0.0678	0.0908	0.1360	0.2710

USGS (2008) Seismic Hazard for -112.45 W, 43.6N						
Period, sec	Frequency, Hz	475 yr p=10% in 50 yr	1,000 yr p=5% in 50 yr	2,500 yr p=2% in 50 yr	10,000 yr p=0.5% in 50 yr	100,000 yr p=.05%in 50 yr
		psrv, cm/sec	psrv, cm/sec	psrv, cm/sec	psrv, cm/sec	psrv, cm/sec
	PGA	0.0600	0.0790	0.1090	0.1800	0.4220
	SA (5%)					
0.0303	33.00	0.2838	0.3736	0.5155	0.8513	1.9959
0.20	5.00	4.8069	6.3055	8.6779	14.2030	32.6825
0.33	3.00	7.0751	9.1565	12.3821	19.5096	43.2854
1.00	1.00	8.2248	10.5820	14.1718	21.2265	42.2969

The site-specific PSHA results have smaller ground motion amplitudes than ground motion determined for the 2008 update of the USGS national hazard maps. USGS PGA estimates are 30% higher at 10^{-3} per year and 40% higher at 10^{-5} per year than amplitudes determined in the site-specific PSHA. The difference in seismic hazard estimates resulted from the following causes.

- The site-specific PSHA used ground motion models for normal slip fault mechanisms; the USGS used various fault mechanisms, or unspecified fault mechanisms, which predict higher amplitude seismic ground motions.
- The weighted result for the site-specific PSHA Includes hazard results for hard rock attenuation models, which leads to lower amplitude seismic ground motions. The USGS 2008 results are for the NEHRP 8-C Boundary site condition which Is a firm rock condition that results in higher amplitude seismic ground motions relative to hard rock site conditions.
- The site-specific PSHA used a local earthquake frequency model determined for the ESRP; the USGS used a larger background seismicity model for the Basin and Range province and a local cell earthquake activity rate that could exceed the historical earthquake rate (Petersen et al., 2008).

Refer to Appendix G for documentation that supports these conclusions.

Site-specific UHRS are compared to USGS 2008 seismic hazard results on Figure 27 for annual probability of exceedance of 10^{-3}. The site-specific and USGS 2008 UHRS are comparable at shorter periods from 0.03 to 0.2 seconds (30 Hz to 5 Hz), with USGS results being higher. USGS results become Increasingly higher than the site specific results at longer periods. This difference Is attributed to usage of hard rock attenuation models in the site-specific PSHA, whereas the USGS 2008 hazard estimates are for a firm bedrock site condition.

Figure 27 provides a comparison of UHRS determined for the INTEC Facility at INL (Payne, 2002) and the site-specific UHRS for exceedance probabilities of 10^{-3} per year and 10^{-4} per year. The INTEC UHRS overlie the site-specific UHRS and have a different spectral shape which is illustrated by a flatter response spectrum. Spectral amplitudes are similar for periods between 0.1 to 0.2 seconds. At lower and higher periods the INTEC UHRS overlie the site-specific UHRS. The difference in response spectra is attributed to the closer proximity of the INTEC facility to the Basin and Range seismic sources and Quaternary Faults located west of INL. The EREF site is located about 48 km (30 mi) east of the INTEC facility at INL. Ground motion models developed for extensional tectonic regimes and used in the site-specific PSHA predict a high rate of amplitude attenuation over relatively short distances for earthquakes associated with normal fault movements.

11.0 References

Ackerman, 2006. A Conceptual Model of Ground-water Flow in the ESRP Aquifer at the Idaho National Laboratory and Vicinity with Implications for Contaminant Transport, U.S. Geol. Surv. Sci. Invest. Report 2006-5122, 62 p., D.J. Ackerman, G.W. Rattray, J.P. Rousseau, L.C. Davis, and B.R. Orr, 2006.

Anders, M.H., Spiegelman, M., Rodgers, D.W., and Hagstrum, J.T., 1993. The Growth of fault-bounded tilt blocks: Tectonics. 11: 1451-1459.

Anderson, S.A. and M.J. Liszewski. 1997. Stratigraphy of the unsaturated zone and the Snake River Plain aquifer at and near the Idaho National Engineering Laboratory, Idaho. United States Geologic Water-Resources Investigations Report. 97-4183.

Anderson, S.A., D.J. Ackerman, M.J. Liszewski, and R.M. Freiburger. 1996a. Stratigraphic data for wells at and near the Idaho National Engineering Laboratory, Idaho. United States Geologic Survey Open-File Report. 96-248.

Anderson, S.A., M.J. Liszewski, and D.J. Ackerman. 1996b. Thickness of surficial sediment at and near the Idaho National Engineering Laboratory, Idaho. United States Geologic Survey Open-File Report. 96-330.

Armstrong, R. L., and others, 1975, K-ar dating, Quaternary and Neocene volcanic rocks of the Snake River Plain, Idaho: Amer. Journal of Science, v. 275, no. 3, p. 225-251.

Armstrong, F.C. and S.S. Oriel. 1965. Tectonic development of Idaho-Wyoming thrust belt. American Association of petroleum Geologists Bulletin. 49-11: 1847-1866.

Blackstone, D.L. 1977. The Overthrust Belt Salient of the Cordillerian Fold Belt. 29th Annual Field Conference – 1977., Wyoming Geological Association Guidebook.

Boore, D.M. and G.M. Atkinson, 2008, *Ground-motion prediction equations for the average horizontal component of PGA, PGV and 5%-damped PSA at spectral periods between 0.01 s and 10 s.*, Earthquake Spectra, Vol. 24, No. 1, pp. 99-138.

Champion, 2002. Accumulation and subsidence of late Pleistocene basaltic lava flows of the eastern Snake River Plain, Idaho, in Link, P.K. and Mink, L.L., eds., Geology, Hydrology, and Environmental Remediation: Idaho National Engineering and Environmental Laboratory, Eastern Snake River Plain, Idaho, Geol. Soc. Amer. Spec. Pap. 353, D.E. Champion, M.A. Lanphere, S.R. Anderson, and M.A. Kuntz, 2002.

Christiansen, 2000. The Quaternary and Pliocene Yellowstone Plateau Volcanic Field of Wyoming, Idaho, and Montana, U.S. Geol. Surv. Prof. Paper 729-G. R.L. Christiansen, 2000.

Christiansen, R.L. and G.F. Embree. 1987. *Island Park, Idaho: Transition from rhyolites of the Yellowstone Plateau to basalts of the Snake River Plain.* Geological Society of American Centennial Field Guide – Rocky Mountain Section. **2:** 103-108.

Christiansen, R.L. and R.A. Hutchinson. 1987. *Rhyolite-basalt volcanism of the Yellowstone Plateau and hydrothermal activity of Yellowstone National Park, Wyoming.* Geological Society of American Centennial Field Guide – Rocky Mountain Section. **2:** 165-172.

Doherty, D. J., L.A. McBroome, and M.A. Kuntz. 1979. *Preliminary geological interpretation and lithologic log of the exploratory geothermal test well (INEL-1), Idaho National Engineering Laboratory, eastern Snake River Plain, Idaho.* United States Geologic Survey Open-File Report. **79-1248.**

Fritz, W.J., and Sears, J.W., 1993, Tectonics of the Yellowstone hotspot wake in southwestern Montana: Geology, v. 21, p. 427-430.

Greeley, 1982. The Snake River Plain, Idaho: Representative of a new category of volcanism, Jour. Geophys. Res., 87, R. Greeley, 1982.

Hackett, 2002. Volcanic hazards of the Idaho National Engineering and Environmental Laboratory, southeast Idaho, in B. Bonnichsen, C.M. White and M. McCurry, eds., Tectonic and Magmatic Evolution of the Snake River Plain Volcanic Province, Idaho Geol. Surv. Bull. 30, W.R. Hackett, R.P. Smith, and S. Khericha, 2002.

Hackett, 1996. Paleoseismology of volcanic environments, in J.P. McCalpin, ed., Paleoseismology, Academic Press, W.R. Hackett, S.M. Jackson, and R.P. Smith, 1996.

Hackett, 1994. Volcanic Hazards of the Idaho National Engineering Laboratory and Adjacent Areas. Idaho National Engineering Laboratory Lockheed Idaho Technologies Company, W. R Hackett and R P. Smith, 1994.

Hackett, 1992. Quaternary Volcanism, Tectonics and Sedimentation in the Idaho National Engineering Laboratory Area. In James It Wilson, ed., Field Guide to Geologic Excursions in Utah and Adjacent Areas of Nevada, Idaho and Wyoming, Utah Geological Survey Miscellaneous Publication 92-3, W. R. Hackett, and R P. Smith, 1992.

Hackett, 1988. Explosive basaltic and rhyolitic volcanism of the eastern Snake River Plain, Idaho, in Link, P.K., and Hackett, W.R., eds., Guidebook to the Geology of Central and Southern Idaho, W.R. Hackett and L.A. Morgan, 1988.

Hughes, 2002. Evolution of Quaternary tholeiitic basalt eruptive centers on the eastern Snake River Plain, Idaho, in B. Bonnichsen, C.M. White and M. McCurry, eds., Tectonic and Magmatic Evolution of the Snake River Plain Volcanic Province, Idaho Geol. Surv. Bull. 30, S.S. Hughes, P.H. Wetmore, and J.L. Casper, 2002.

Hughes, S.S., R.P. Smith, W.R. Hackett, and S.R. Anderson. 1999. *Mafic volcanism and environmental geology of the eastern Snake River Plain, Idaho. In:* S.S. Hughes and G.D. Thackray. Eds. *Guidebook to the geology of eastern Idaho:* Idaho Museum of Natural History. 143-168.

Hyndman, D. W., 1983, The Idaho batholith and associated plutons, Idaho and Western Montana, *in* Roddick, J. A., editor, Circum-Pacific Pluntonic Terranes: Geologic Society of America Memoir 159, 213-240.

Idaho Department of Natural Resources (IDNR). 2002. *Well Costruction Search.* http://www.idwr.idaho.gov/apps/appswell/searchWC.asp.

Idaho National Laboratory at http://www.inl.gov/geosciences/earthquakes.shtml, Earthquake information accessed on June 16, 2008.

Janecke, S.U.. 1994. *Sedimentation and paleogeography of an Eocene to Oligocene rift zone, Idaho and Montana:* Geological Society of America Bulletin, **106:** 1083-1095.

Janecke, S.U. 1993. *Structures in segment boundary zones of the Lost River and Lemhi faults, east-central Idaho:* Journal of Geophysical Research. **98:** 16,223-16,238.

Janecke, S.U. 1992. *Kinematics and timing of three superposed extensional systems, east central Idaho: Evidence for an Eocene tectonic transition:* Tectonics. **11:** 1121-1138.

Kellogg, K.S., D.W.Rodgers, F.R. Hladky, M.A. Kiessling, and J.W Riesterer. 1999. *The Putnam Thrust Plate, Idaho.Dismemberment and tilting by Tertiary normal faults, In*: Hughes, S.S., and Thackray, G.D., eds., Guidebook to the Geology of Eastern Idaho: Pocatello, Idaho Museum of Natural History. 97-114

Kuntz, 2002. Tension cracks, eruptive fissures, dikes and faults related to late Pleistocene – Holocene basaltic volcanism and implications for the distribution of hydraulic conductivity in the eastern Snake River Plain, Idaho, in Link, P.K. and Mink, L.L., eds., Geology, Hydrology, and Environmental Remediation: Idaho National Engineering and Environmental Laboratory, Eastern Snake River Plain, Idaho, Geol. Soc. Amer. Spec. Pap. 353, M.A. Kuntz, S.R. Anderson, D.E. Champion, M.A. Lanphere, and D.J. Grunwald, 2002.

Kuntz, 1994. Geologic Map of the Idaho National Engineering Laboratory and Adjoining Areas, eastern Idaho, U.S. Geol. Surv. Misc. Inv. Map I-2330, M.A. Kuntz, B. Skipp, M.A. Lanphere, G.B.

Dalrymple, D.B. Champion, G.F. Embree, W.R. Page, L.A. Morgan, R.P. Smith, W.R. Hackett, and D.W. Rodgers, 1994.

Kuntz, 1992a. A model-based perspective of basaltic volcanism, eastern Snake River Plain, Idaho, in Link, P.K., Kuntz, M.A., and Platt, L.B., eds., Regional Geology of Eastern Idaho and Western Wyoming, Geological Society of America Memoir 179, M.A. Kuntz, 1992.

Kuntz, 1992b. An overview of basaltic volcanism of the eastern Snake River Plain, Idaho, in Link, P.K., Kuntz, M.A., and Platt, L.B., eds., Regional Geology of Eastern Idaho and Western Wyoming, Geological Society of America Memoir 179, M.A. Kuntz, H.R. Covington, and L.J. Schorr, 1992.

Kuntz, 1988. Geologic map of the Craters of the Moon, Kings Bowl, and Wapi lava fields, and the Great Rift volcanic rift zone, south-central Idaho, U.S. Geol. Surv. Misc. Inv. Map I-1632, M.A. Kuntz, D.E. Champion, R.H. LeFebvre, and H.R. Covington, 1988.

Kuntz, 1986. Radiocarbon studies of latest Pleistocene and Holocene lava flows of the Snake River Plain, Idaho: Data, lessons, interpretations, Quat. Res., 25, M.A. Kuntz, E.C. Spiker, M. Rubin, D.E. Champion, and R.H. LeFebvre, 1986.

Kuntz, 1979. Geology, geochronology and potential volcanic hazards in the Lava Ridge – Hells Half Acre area, eastern Snake River Plain, Idaho, U.S. Geol. Surv. Open-File Report 79-1657, M.A. Kuntz and G.B. Dalrymple, 1979.

Kuntz, 1978. Geology of the Arco – Big Southern Butte area, eastern Snake River Plain, and potential volcanic hazards to the Radioactive Waste Management Complex and other waste storage and reactor facilities at the Idaho National Engineering Laboratory, Idaho, U.S. Geol. Surv. Open-File Rep. 78-691, M.A. Kuntz, 1978.

Link, P.K. and S.U. Janecke. 1999. *Geology of east-central Idaho: Geologic roadlogs for the Big and Little Lost River, Lemhi and Salmon River Valleys. In:* S.S. Hughes and G.D. Thackray. Eds. *Guidebook to the geology of eastern Idaho:* Idaho Museum of Natural History. 295-234.

Monley, Lawrence E., 1971, Petroleum Potential of the Idaho-Wyoming Overthrust Belt, Am. Assoc. Petroleum Geologists Memoir 15, p. 509-529.

Parsons, T., G.A. Thompson, and R.P. Smith. 1998. *More than one way to stretch a tectonic model for extension along the plume track of the Yellowstone hotspot and adjacent Basin and Range Province.* Tectonics. **17-2:** 221-234.

Parsons, T. and G.A. Thompson. 1991. *The Role of Magma Overpressure in Suppressing Earthquakes and Topography: Worldwide Examples.* Science. **253-5023:** 1399-1402.

Payne, S.J., V.W. Gorman, S.A. Jensen, M.E. Nitzel, M.J. Russell, and R.P. Smith, 2002, *Development of Probabilistic Design Basis Earthquake (DBE) Parameters for Moderate and High Hazard Facilities at INEEL*, INEEL/EXT-99-00775, Final Report Revision 2, June 2002.

Petersen, M.D., A.D. Frankel, S.C. Harmsen, C.S. Mueller, K.M. Haller, R.L. Wheeler, R.L. Wesson, Y. Zeng, O.S. Boyd, D.M. Perkins, N. Luco, E.H. Field, C.J. Willis, and K.S. Rukstales, 2008. *Documentation for the 2008 Update of the United States National Seismic Hazard Maps*, US Geological Survey, Open-File Report 2008-1128.

Rodgers, D.W., and Anders, M.H., 1990, Neogene evolution of Birch Creek Valley near Lone Pine, Idaho, *in* Roberts, Sheila, ed., Geologic field tours of western Wyoming and parts of adjacent Idaho, Montana, and Utah: Geological Survey of Wyoming Public Information Circular no. 29, p. 26-38.

Sanford, R.F. 2005. *Geology and stratigraphy of the Challis Volcanic Group and related rocks, Little Wood River are, south-central Idaho.* Unites States Geologic Survey Bulletin. **2064-II.**

Sears, J. W., and Fritz, W. J., 1998, *Cenozoic tilt domains in southwestern Montana: Interference among three generations of extensional fault systems, In:* Faulds, J. E., and Stewart, J. H., eds., *Accommodation zones and transfer zones: The Regional segmentation of the Basin-and-Range Province,* Geological Society of America Special Paper 323, p. 241-249.

Shoemaker, K.A. and W.K. Hart. 2002. *Temporal controls on basalt genesis and evolution on the Owyhee Plateau, Idaho and Oregon. In:* C.M. White and M. McCurry. Eds. *Tectonic and magmatic evolution of the Snake River Plain volcanic province: Idaho.* Geological Survey Bulletin. **30:** 313-328.

Smith, R.P. 2004. *Geologic Setting of the Snake River Plain Aquifer and Vadose Zone.* Vadose Zone Journal. **3:** 47-58.

Spudich, P., J.B. Fletcher, M. Hellweg, J. Boatwright, C. Sullivan, W.B. Joyner, T.C. Hanks, D.M. Boore, A. McGarr, L.M. Baker, and A.G. Lindh, 1997, *SEA97 – A new predictive relation for earthquake ground motions in extensional tectonic regimes*, Seismological Research Letters, v. 68, p. 190-198.

Spudich, P., J.B. Fletcher, M. Hellweg, J. Boatwright, C. Sullivan, W.B. Joyner, T.C. Hanks, D.M. Boore, A. McGarr, L.M. Baker, and A.G. Lindh, 1999, *SEA99 – A revised ground motion prediction relation for use in extensional tectonic regimes*, Bulletin of the Seismological Society of America, v. 89, p. 1156-1170.

US Geological Survey Earthquake Hazards Program, 2008, http://earthquake.usgs.gov/research/hazmaps/products_data/2008/hazardvalues/, Earthquake information accessed on June 9, 2008.

US Geological Survey Earthquake Hazards Program, 2002, http://earthquake.usgs.gov/research/hazmaps/products_data/2002/data2002.php, Earthquake information accessed on June 9, 2008.

Vetter, S., J. Shervais, and M. Zarnetske. 2005. *Basaltic volcanism in the western Snake River Plain and Boise River Valley: ferrobasalts, flotation cumulates, and the change to K-rich ocean island basalts 750,000 years ago.* Geological Society of America Abstracts with Programs. **37-7:** 127.

Wetmore, P.H., S.S. Hughes, D.W. Rodgers, and S.R. Anderson. 1999. *Late Quaternary constructional development of the axial volcanic zone, eastern Snake River Plain, Idaho*: Geological Society of America Abstracts With Programs. **31-4:** A-61.

Womer, 1982. Phreatic eruptions of the eastern Snake River Plain of Idaho, in B. Bonnichsen and R.M. Breckenridge, eds., Cenozoic Geology of Idaho, Idaho Bur. Mines Geol. Bull. 26, M.B. Womer, R. Greeley, and J.S. King, 1982.